

NASA  
CR  
3216  
c.1

NASA Contractor Report 3216

TECH LIBRARY KAFB, NM  
0062092

# Premixing Quality and Flame Stability A Theoretical and Experimental Study

Krishnan Radhakrishnan, John B. Heywood,  
and Rodney J. Tabaczynski

GRANT NGR 22-009-378  
DECEMBER 1979

**NASA**



NASA Contractor Report 3216

# Premixing Quality and Flame Stability: A Theoretical and Experimental Study

Krishnan Radhakrishnan, John B. Heywood,  
and Rodney J. Tabaczynski  
*Massachusetts Institute of Technology  
Cambridge, Massachusetts*

Prepared for  
Lewis Research Center  
under Grant NGR 22-009-378

**NASA**

National Aeronautics  
and Space Administration

**Scientific and Technical  
Information Branch**

1979



## TABLE OF CONTENTS

		Page
1	INTRODUCTION . . . . .	1
2	BLUFF BODY FLAME STABILIZATION: A BRIEF REVIEW . . . . .	4
	2.1 Aerodynamics of Bluff Body	
	Flame Stabilization . . . . .	4
	2.2 Blowoff Experiments . . . . .	6
3	BLOWOFF VELOCITY CORRELATION BASED ON COHERENT	
	TURBULENT STRUCTURES . . . . .	8
	3.1 Coherent Turbulent Structures . . . . .	8
	3.2 Correlation for the Blowoff Velocity . . . . .	10
	3.3 Laminar Flame Speed Correlation . . . . .	12
	3.4 Comparison of Blowoff Velocity	
	Correlation with Published Data . . . . .	13
4	A STOCHASTIC MIXING MODEL FOR MODELLING	
	FLAME IGNITION AND BLOWOUT . . . . .	22
	4.1 A Statistical Model with Monte	
	Carlo Mixing . . . . .	22
	4.2 Computational Procedures . . . . .	25
	4.3 Results and Discussion . . . . .	26
	4.3.1 Parametric Studies for	
	Uniform Mixtures . . . . .	26
	4.3.2 Effect of Mixture Nonuniformity	
	on the Lean Ignition Limit . . . . .	30
5	EXPERIMENTAL APPARATUS AND PROCEDURES . . . . .	32
	5.1 Experimental Hardware . . . . .	32
	5.2 Gas Analysis Equipment . . . . .	35
	5.3 Instrumentation . . . . .	35
	5.4 Safety Features . . . . .	37
	5.5 Experimental Procedures . . . . .	37
	5.5.1 Fuel and Equivalence Ratio	
	Determination . . . . .	37
	5.5.2 Lean Ignition Limit . . . . .	37
	5.5.3 Lean Blowout Limit . . . . .	39
	5.6 Operating Parameters . . . . .	41
6	RESULTS AND DISCUSSION . . . . .	43
	6.1 Measured Species Concentrations . . . . .	43
	6.2 Lean Ignition and Blowout Limits:	
	Parametric Study and Comparison with	
	Model Predictions . . . . .	48
7	CONCLUSIONS . . . . .	52
	REFERENCES . . . . .	54

## 1 INTRODUCTION

To control pollution from aero-engines generated in and around airports the United States Environmental Protection Agency (EPA) has promulgated emission standards for aircraft gas turbine engines. Also, the introduction of emissions, particularly  $\text{NO}_x$  (oxides of nitrogen), into the stratosphere is an area of current concern. In the Climatic Impact Assessment Report (1),  $\text{NO}_x$  were identified as key pollutant emissions during high altitude flight of both subsonic and supersonic aircraft. Preliminary findings suggested that substantial reductions in  $\text{NO}_x$  need to be achieved to avoid ozone depletion of the stratosphere with consequent increases in sea-level radiation. The Climatic Impact Assessment Program recommended six- to ten-fold reductions in  $\text{NO}_x$  below current levels. To meet these emissions standards and cruise objectives, several advanced combustor concepts are being developed. Combustion in a gas turbine engine represents a unique problem with regard to the control of the production of  $\text{NO}_x$ . The  $\text{NO}_x$  is produced as a result of reactions involving either molecular oxygen (with atomic nitrogen) or molecular nitrogen (with atomic oxygen). The extreme stability of these molecules implies that reactions involving either atomic oxygen or atomic nitrogen become important only at high temperatures. However, in a gas turbine engine, the air is compressed before it is mixed with the fuel and burned, resulting in high temperature levels in the combustion zone. This makes the conventional gas turbine combustion process particularly prone to the formation of  $\text{NO}_x$ .

One new combustor concept with the potential for very low  $\text{NO}_x$  emissions is the lean premixed-prevaporized system (2). This idea, suggested in references 3 and 4 is basically simple: since the  $\text{NO}_x$  formation process is extremely temperature sensitive, reductions in the local flame temperature achieved with little or no sacrifice in the combustion efficiency should result in substantial reduction in emissions. A key feature of this technique is the attainment of complete evaporation of the fuel, and complete mixing of the fuel and air before combustion. By operating the primary combustion region at an equivalence ratio substantially leaner than stoichiometric,  $\text{NO}_x$  emissions should be substantially reduced. This technique has been shown to be effective in reducing thermal  $\text{NO}_x$  emissions (5-9). For example, Anderson (5,6) showed that by leaning out the combustion zone, an order of magnitude reduction in  $\text{NO}_x$  is achieved while still maintaining 99 percent combustion efficiency. He obtained an emission index of between 0.3 and 1.0 g  $\text{NO}_2/\text{kg}$  fuel; values for conventional combustors are in the range 3 - 20 g  $\text{NO}_2/\text{kg}$  fuel.

Although the technique of premixing and prevaporizing shows great promise for reducing  $\text{NO}_x$  emissions levels, there are several problems associated with the practical application of this concept (2). This report addresses two of these problems: (i) the avoidance of blowout and (ii) altitude relight. For lean premixed flows combustion stability is poor and blowout occurs at much lower flow velocities than for stoichiometric mixtures (10). Thus, while mixture uniformity reduces  $\text{NO}_x$  emissions, it makes the desired combustor stability limits much harder to achieve. In a conventional combustor, the mean fuel-air ratio can be less than the lean flammability limit and locally richer than average

zones will help maintain stable combustion. For the uniform mixture combustion that results from premixing, this advantage is lost and blowout will occur near the lean flammability limit.

This report examines the effects of fuel-air ratio nonuniformities on flame stability in (fuel) lean fuel-air mixtures. More specifically, this study examines the effects of premixing quality on the lean ignition and blowout limits in a simple tubular combustor. This work has involved both theoretical and experimental investigations. Although the effects of fuel-air mixture nonuniformities on the production of  $\text{NO}_x$  are well understood (e.g. reference 11), little is known about their effects on flame stability. Nearly all the theoretical and experimental research relating to turbulent flame propagation has been concerned with premixed flames and application to real combustors is limited (12).

In the modeling phase, a correlation for the blowoff velocity of premixed turbulent flames has been developed using the concept of coherent turbulent structures. The model uses the basic quantities of a turbulent flow; i.e. the integral length scale, the Taylor microscale, the Kolmogorov length scale, and the turbulent intensity. The model identifies the laminar burning of the fuel-air mixture across the microscale as being the critical process for turbulent flame stabilization. The correlation is based on a Karlovitz analysis where two characteristic times - a chemical time and a flow time - are identified, and compared with each other. The ratio of these two times defines a limiting value at which a flame will no longer propagate. The blowoff velocities predicted by the correlation are shown to be in good agreement with experimental data.

In order to investigate the effects of fuel-air ratio nonuniformities on the lean ignition limit, a stochastic mixing model with chemical reaction based on the work of Flagan and Appleton (13) has been developed. In this model, the recirculation zone downstream of the flameholder is treated as a partially stirred reactor. The composition of the recirculation zone is described by an ensemble of (N) equal mass fluid elements which have a distribution of thermodynamic states. The major inputs into the model are the characteristic size of the reactor, the reference velocity and the residence time. These inputs define a mixing frequency which determines the frequency at which these (N) elements interact, and a removal rate determined by the residence time. The model allows for nonuniformities in mixture composition and involves a minimum of geometric variables.

This model has been used to predict the lean ignition and blowout limits of fully premixed systems. To simulate the ignition process, a few elements are ignited at time  $t = 0$ , and the properties of the ensemble are calculated as a function of time. Successful ignition is characterized by a growth in the ensemble burnt fraction. The blowout process is simulated by igniting most of the elements at time  $t = 0$ ; blowout is characterized by the ensemble burnt fraction continuously decreasing with time to approach zero. Using an assumed distribution to describe the fuel fraction distribution entering the recircu-

lation zone, the effect of mixture nonuniformity on the lean ignition limit is studied.

The experimental work was carried out in an atmospheric pressure tubular combustor. The experimental facility consisted of an air-heater, a fuel premixing section constructed in modules so the premixing length could be varied, a perforated plate flame stabilizer, and a combustion section. The fuel used was gaseous propane. Thus, an idealized combustion situation was created which did not include the effects of droplet evaporation, dilution air etc., which are present in gas turbine combustors. In this way the variables of interest were isolated so that their effects on flame stability could be studied at a fundamental level.

In Section 2 the underlying concepts of flame stabilization are reviewed. The correlation of the blowoff velocity of premixed turbulent flames is derived in Section 3. In Section 4 the statistical mixing model for flame ignition and blowout is described. The next section, 5, describes the experimental apparatus and procedures. The results from the modelling and experimental efforts are presented and compared in Section 6. The conclusions based on these findings are presented in Section 7.

## 2 BLUFF BODY FLAME STABILIZATION: A BRIEF REVIEW

Flame stabilization is of fundamental importance in the design, efficient performance and reliable operation of high speed propulsion systems. In gas turbines and other combustion equipment, the velocities at which the gases flow are much higher than the maximum flame speeds of practical fuels. Therefore, an ignition energy source and regions of low velocity must be provided within the combustor to stabilize or anchor the flame. There are several techniques for stabilizing turbulent flames; we shall restrict our discussion to the use of bluff bodies. Longwell (14, 15), Penner and Williams (16), Williams (17) and Ozawa (18) discuss this and other techniques of flame stabilization in high speed combustion systems.

The technique of stabilizing flames by means of bluff bodies (such as vee gutters and disks) placed in the main flow is not new. As early as 1943, Wolfhard (19) observed flame stabilization on a cylindrical obstacle. He showed that the blowoff velocity -- defined as the approach velocity above which a flame cannot be stabilized by the flameholder -- was dependent on the cylinder diameter and pressure for a given combustible mixture. Since then, several investigators have measured the variation of blowoff velocity with flameholder shape and size, inlet temperature, inlet pressure, etc., (20 - 39).

Most flame stabilizing techniques exploit a recirculating type of flow for anchoring the flame. Flame stabilization phenomena represent a complex interaction between fluid mechanic and chemical reaction processes; however, this aerodynamic flow structure is common to all forms of wake stabilized flames.

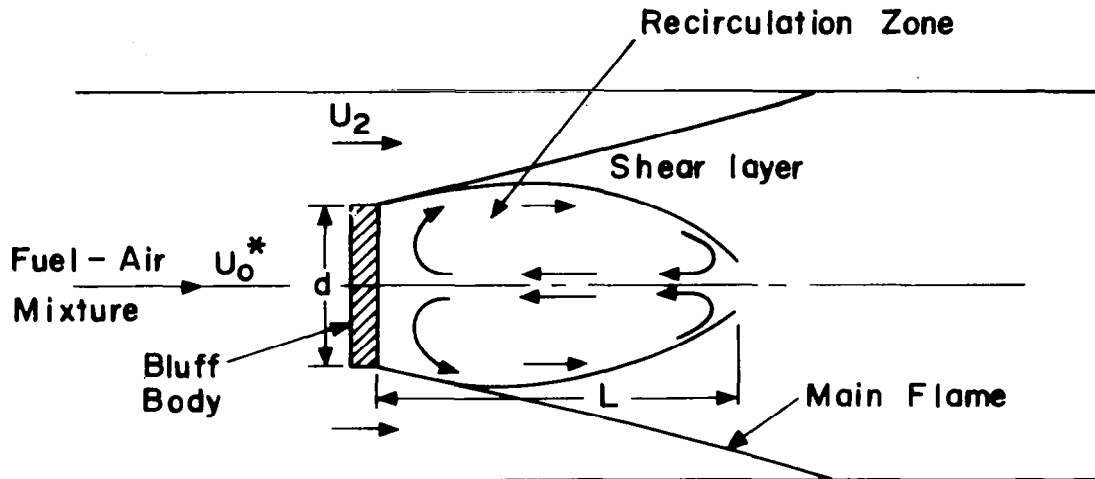
### 2.1 Aerodynamics of Bluff Body Flame Stabilization

Figure 1 shows a schematic of the wake flow immediately downstream of a typical bluff body flame stabilizer. This wake consists of a backflow (i.e. recirculating) region bounded by free shear layers. In practical combustion systems, the main stream flowing over the flameholder and the free shear layer are turbulent. Mass, momentum and energy are exchanged across the turbulent mixing layer; however, a boundary of zero net mass exchange exists within the shear layer.

The presence of the recirculation zone is essential for bluff body flame stabilization. The recirculation zone serves as a continuous source of energy and active species for igniting the fresh combustible mixture. Toong (40) lists the essential features for bluff body flame stabilization.

Several different techniques have been used for observation of the recirculation zone, both with and without combustion; for details of these techniques see references 18, 19, 22, 25, 32-34, 41. These studies confirmed the existence of the backflow region immediately downstream of the stabilizer. Although there was some evidence of vortex shedding (Karman vortex street) before ignition (i.e. in cold flow), no vortex shedding was observed during





\* At Blowoff,  $U_0 = U_b$

Figure 1 Schematic of a Bluff Body Stabilized Flame.

combustion. The presence of the flame inhibits vortex shedding. The upstream motion was observed to occur randomly throughout the wake flow.

Several investigators (e.g. 24, 25, 33, 34, 38, 39, 41) have measured the length ( $L$ ) of the recirculation zone, both in cold and in hot flow. The presence of the flame causes an increase in the volume and length of the recirculation zone. These investigations showed that the ratio  $L/d$  is constant (with and without combustion) for sufficiently high Reynolds numbers ( $U_0 d/\nu$ ). Moreover,  $L$  was found to be practically constant over a wide range of equivalence ratios. Although the ratio  $L/d$  was found to increase with combustion, the maximum diameter of the recirculation zone boundary was unchanged. This diameter was found to be constant over a wide range of equivalence ratios, inlet velocities and blockage due to the flameholder.

Winterfield (38) and Bovina (41) measured the residence times behind flameholders. The residence time is the average time a fluid particle stays in the recirculation zone. These studies showed that the residence times (for both cold and hot flows) varied directly with the characteristic size ( $d$ ) of the flameholder and inversely with the velocity ( $U_0$ ). Increasing flameholder blockage resulted in a decrease in the residence time. With combustion, the residence time increases. The residence time  $\tau_r$  can therefore be expressed in terms of  $d$  and  $U_0$  as follows:

$$\tau_r = \kappa d / U_o$$

where  $\kappa$  is a constant that depends on the flameholder blockage and whether the flow is isothermal or combusting. Assuming sufficiently high Reynolds numbers so that  $L \propto d$ , the above equation can be rewritten as

$$\tau_r = c_\tau L / U_o$$

where  $c_\tau$  has absorbed the ratio  $d/L$ .

## 2.2 Blowoff Experiments

Blowoff experiments are of direct practical interest because they determine the maximum flow rates at which a flame can be stabilized. Observations of the sequence of events which occur during blow off (22, 23, 25) show that the flame is first extinguished downstream and that the point of extinction then moves upstream to the flameholder. For approach velocities close to the blowoff limit, the main flame region disappears, leaving only a small region of burning immediately downstream of the flameholder. A small increase in the velocity causes complete extinguishment of the flame.

We conclude this section with a summary of the qualitative effects of various parameters on the blowoff limit; a quantitative discussion of these effects follows in Section 3.4. Exclusive of the mixture stoichiometry and velocity, these parameters are: (a) Fuel type: Stability is favored by a decrease in the minimum spark ignition energy and an increase in the normal burning velocity of the combustion mixture (28). (b) Mixture temperature: Increases in inlet temperature lead to faster burning rates and hence an increase in stability (24, 27, 30). (c) Combustor pressure: The work of Scurlock (22) and DeZubay (26) showed that decreasing pressure has a detrimental effect on stability. However, enclosed flames are prone to pressure fluctuations which can cause a large reduction in the stability (14) (see (h) below). However, Longwell et al (24) and, more recently, Roffe and Venkatramani (42, 43) found little or no pressure dependence up to 30 atmospheres. The exact effect of pressure is therefore unclear. (d) Stabilizer type: In general, a two-dimensional stabilizer (cylinder across a rectangular duct) has better stability characteristics than a three-dimensional flameholder (disk or sphere in a duct) of the same characteristic dimension (28). (e) Flameholder shape: Very little effect of baffle shape is reported. Scurlock (22) and Longwell et al (24) showed that changes in the baffle shape had little or no effect on the blowoff velocity. However, Longwell et al (24) found that streamlining the trailing edge of the baffle (thereby reducing its 'bluffness') had a detrimental effect on the stability. (f) Flameholder size: In general, an increase in the characteristic size of the flameholder leads to an increase in the range of stable operation (e.g. (26)). But, as the dimensions of the combustion chamber and of the stabilizer become of comparable magnitude, the stability decreases with increasing characteristic dimension of the stabilizer (28,44). Thus, an optimum flameholder size exists for a given combustion chamber. Friedman et al (44)

found the optimum value of blockage for an annular V-gutter in a circular duct to be in the vicinity of 30 to 40 percent. (g) Flameholder temperature: Increases in flameholder temperature increase the stability (28, 29). However, the magnitude of the variation depends on the inlet velocity (29) and the characteristic dimension (45), being insignificant in some cases. (h) Acoustic effects: The general conclusion is that increasing noise intensity decreases the stability (14, 15, 28, 35). (i) Combustor length: Decreasing the distance downstream of the flameholder over which the flame is confined decreases the noise intensity and hence improves stability (15, 28). But, Scurlock (22) found that decreasing the length beyond a certain limit had a detrimental effect on stability. (j) Turbulence of the entering stream: Increasing the incoming stream turbulence decreases the stability. However, for large stabilizers, the effect of approach stream turbulence is not significant (14, 22, 23, 28).

### 3 BLOWOFF VELOCITY CORRELATION BASED ON COHERENT TURBULENT STRUCTURES

In this section, a correlation for the blowoff velocity of premixed turbulent flames stabilized by bluff bodies is derived using the concept of coherent turbulent structures\*. Before a model for the combustion process can be developed, it is necessary to assume that a specific turbulence structure exists in the combustion zone. The major parameters of interest are the turbulent intensity and the integral length scale. In this analysis, the turbulence structure is assumed to be coherent, and the isotropic relationships for defining the various length scales are assumed to be valid.

#### 3.1 Coherent Turbulent Structures

In recent years there has been a growing interest in studying the large-scale coherent structures that are found in shear-flow turbulence. For example, Brown and Roshko (46,47,48) have demonstrated experimentally the existence of organized vortex structures in a turbulent mixing layer. Other examples where orderly eddy structures have been clearly identified are discussed by Davies and Yule (49) (and others (50-52)) in their review on coherent structures in turbulence.

The existence of these large-scale well-defined (i.e. coherent) structures or eddies has prompted several researchers to propose turbulent combustion models based on the existence of these structures. For example, Chomiak (53), Tabaczynski et al (54), and Spalding (55) have presented combustion models based on these coherent large-scale eddies. Tabaczynski et al (54) used the concept of coherent structures to construct an entrainment model for turbulent combustion in spark-ignition engines. Hires et al (56) found good agreement between the predictions made by this model of the ignition delay and combustion duration in spark ignition engines and experimental data, for three different engine geometries. The models developed by Chomiak (53) and Tabaczynski et al (54) emphasize the importance of the internal structure of the large-scale eddy to the combustion process.

Townsend (57), Corrsin (58) and Tennekes (59) have suggested models for the geometry of the small-scale (or fine) structure of turbulence. Townsend (57) suggested that the smallest scale components (smaller than the Kolmogorov microscale) can be modelled as sheets or lines of vorticity passively superimposed on the main turbulence field. In Corrsin's model, the energy dissipation was localized in randomly distributed thin sheets (or slabs). He assumed a slab thickness of the order of the Kolmogorov scale and spacing of the order of the integral scale. Tennekes modified this idea by suggesting a model of randomly distributed vortex tubes with diameter on the order of the Kolmogorov scale and average spacing of the Taylor microscale, Figure 2. Kuo and Corrsin (60, 61) investigated experimentally the geometry of the small regions in which

---

\*

The velocity referred to here is the maximum velocity for which the flame continues to propagate into the main stream -- see section 2.2 for a description of the sequence of events which occurs during blowoff.

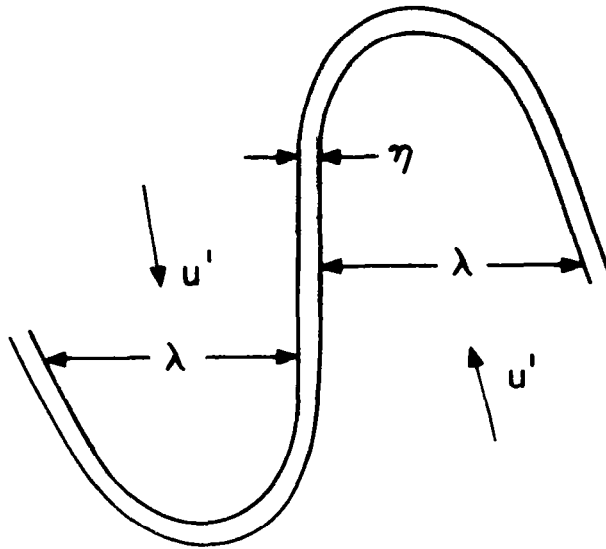


Figure 2 Schematic of Small-Scale Structure Proposed by Tennekes (59).

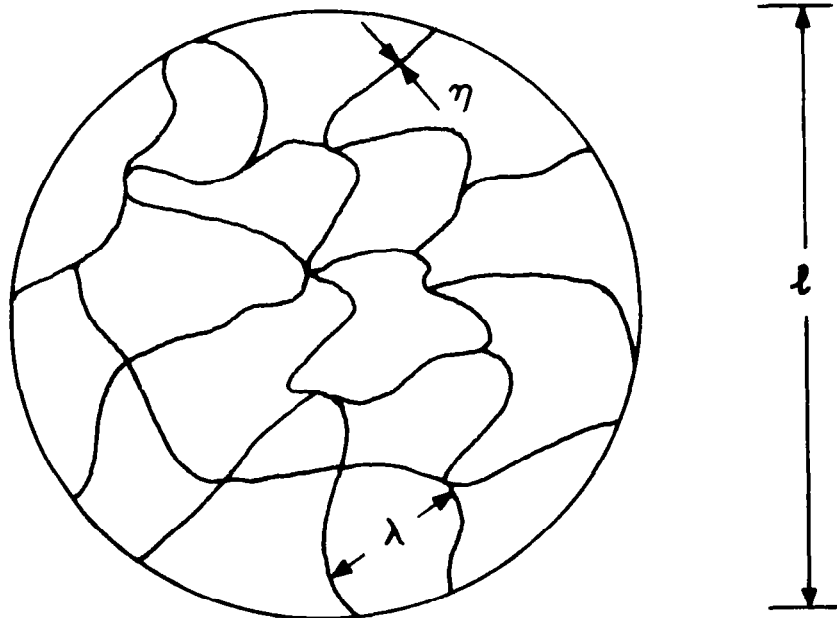


Figure 3 Schematic of Large-Scale Structure Proposed by Tabaczynski et al (54).

the fine-scale structure is active. Their conclusion was that the small-scale structures are typically ribbons or tubes of vorticity. The model (for the geometry of the small-scale structure) that comes closest to their data was that proposed by Tennekes (59).

This view of the internal structure of the large-scale eddy has been adopted by Chomiak and Tabaczynski et al. The basic structure proposed by Tabaczynski et al is shown in Figure 3. This figure shows the internal structure of a single turbulent eddy of integral scale  $\ell$ . This length scale defines the characteristic size of the large-scale structure. The Kolmogorov or dissipation scale  $\eta$  is assumed to be the scale of the vortex tubes. This model gives a physical meaning to the Taylor microscale  $\lambda$ . It is defined as the average spacing of the randomly distributed vortex tubes (see Tennekes (59) and Figure 2).

The idealized eddy structure proposed by Tabaczynski et al (54) is used next to derive a correlation for the blowoff velocity of premixed turbulent flames stabilized by bluff bodies.

### 3.2 Correlation for the Blowoff Velocity

The idealized eddy structure shown in Figure 3 defines characteristic length and velocity scales used in this model of turbulent combustion. The structure is characterized by the size of the structure  $\ell$  generally called the integral scale, the dissipation or Kolmogorov scale,  $\eta$ , and the spacing of the vortex tubes,  $\lambda$ . The microscale  $\lambda$  plays a major role; it is the scale over which laminar burning takes place. The Kolmogorov scale  $\eta$  is significant in this model in that it is the scale over which combustion proceeds very rapidly once the flame has been initiated; ignition sites are assumed to be carried along the vortex tubes at a rate  $u' + S_L$ , where  $u'$  is the turbulent intensity and  $S_L$  the laminar flame speed of the fuel-air mixture. The turbulent intensity is therefore being interpreted as the local velocity of a vortex tube along its axis (see Figure 2).

These concepts can be used to define characteristic chemical and flow times. The chemical time is defined to be the time characteristic of burning on the microscale  $\lambda$ , and is given by

$$\tau_c = \lambda / S_L \quad (1)$$

Using the definition for isotropic turbulence,  $\lambda$  can be written in terms of  $\ell$  (see Tennekes and Lumley (62)).

$$\lambda = (15/A)^{1/2} \ell (u' \ell / \nu)^{-1/2} \quad (2)$$

where  $A$  is a constant of order unity.

This analysis assumes that the isotropic relationships for defining the length scales are valid within a single eddy. The tendency towards isotropy in the small scales is well known (47). But the large-scale turbulence behind

flameholders is thought to be non-homogeneous (18). However, the assumption of homogeneous, isotropic turbulence is adequate here in view of the relative simplicity of the combustion model and also in view of the meagre information available on the turbulence characteristics of bluff bodies.

For the flow (or mixing) time, the characteristic eddy time  $\tau_e$  is used:

$$\tau_e = \ell/u' \quad (3)$$

These characteristic chemical and flow times can be used to develop a correlation for the blowoff velocity of premixed turbulent flames stabilized by bluff bodies. A ratio  $R_\tau$

$$R_\tau = \tau_c/\tau_e \quad (4)$$

is defined which determines the limiting value at which a flame will continue to propagate. Using equations (1) - (3), equation (4) can be rewritten as

$$R_\tau = \left( \frac{15}{A} \right)^{1/2} \frac{(u'v/\ell)^{1/2}}{S_L} \quad (5)$$

where A is a constant of order unity.

If we further make the assumptions that  $u' = C_1 U_2$  where  $U_2$  is the velocity at blowoff, in the plane of maximum flameholder blockage, and  $\ell = C_2 L$ , where L is the length of the recirculation zone (see Figure 1) and  $C_1$  and  $C_2$  are constants, equation (5) can be rewritten as

$$R_\tau = (U_2 v/L)^{1/2} / S_L$$

or

$$U_2 = R_\tau^2 S_L^2 L/v \quad (6)$$

where  $R_\tau$  has absorbed all the unknown constants.

For given flameholder and combustor geometries, the approach velocity  $U_b$  (Figure 1), can be related to the velocity  $U_2$  in the plane of the flameholder by means of the continuity equation. For incompressible, isothermal flow of the fuel-air mixture, this relation takes the form\*

$$U_b = U_2 (A_o/A_c) = U_2 (1 - R_B) \quad (7)$$

\* We are neglecting the slight preheating of the fuel-air mixture as it flows past the flameholder. For very high blockage ratios and velocities, compressibility effects must also be included.

where  $A_o$  is the open area of the flameholder,  $A_c$  is the cross-sectional area upstream of the flameholder and  $R_B$  is the flameholder blockage ratio ( $= 1 - A_o/A_c$ ).

The substitution of equation (7) into equation (6) yields

$$U_b = R_1^2 S_L^2 L/\nu \quad (8)$$

where  $R_1^2$  has absorbed the ratio  $A_o/A_c$ . We note here that although  $R_1$  can vary from one flameholder-combustor combination to another, it is constant for fixed flameholder and combustor geometries.

This theory indicates that the blowoff velocity of a bluff body stabilized flame is proportional to the square of the laminar flame speed of the fuel-air mixture times the length of the recirculation zone (which, for large enough Reynolds numbers based on the free stream velocity, characteristic size of the flameholder and state of the combustible stream, is known to be directly proportional to the size (d) of the flameholder -- see Section 2.1). Equation (8) can be interpreted as a flame stability requirement as follows: the characteristic time for burning on the micro-scale must be shorter than the eddy time. The model, therefore, identifies laminar burning of the fuel-air mixture over the microscale  $\lambda$  as being the critical process.

This laminar flame speed dependence has been proposed by others (63-66). To prove this dependence on the laminar flame speed, Loblich (66) performed experiments at constant pressure, constant unburnt temperature and approximately equal values of the Reynolds number  $U_b d/\nu$  on cylindrical flameholders. From these results it was shown that the term  $U_b/LS_L^2$  is constant.

### 3.3 Laminar Flame Speed Correlation

The blowoff velocity of premixed turbulent flames stabilized by bluff bodies was shown to be proportional to the square of the laminar flame speed (equations (6) and (8)). In order to study the variation of the blowoff velocity (for a given fuel) with the fuel-air equivalence ratio ( $\phi$ ), inlet temperature ( $T_u$ ) and pressure ( $p_u$ ), it is necessary to know the variation of the flame speed with these parameters. However, there is a general lack of flame speed data for high temperatures and pressures.

There is a wide scatter in the published values of the burning velocity. In their review on the measurement techniques of the laminar flame speed, Andrews and Bradley (67) report that, even for a relatively simple fuel, methane, there is considerable scatter in the published values of the maximum burning velocity. For a pressure and unburnt temperature of 1 atmosphere and 298 K respectively they found a data scatter of over 25 percent in the maximum burning velocity of methane-air mixtures. They concluded that these discrepancies were dependent to some extent on the experimental technique. This data scatter tends to widen for equivalence ratios away from unity. Andrews and Bradley (68) attribute this increase to the rapid increase in both the



quenching distance and the flame thickness as the flammability limits are approached. In a recent survey of existing data on laminar flame speeds, Lavoie (69) concludes that existing data at high pressures are restricted to near stoichiometric fuel-air mixtures.

Since there are considerable discrepancies in the literature on the measured laminar flame speeds, we have used the correlation formula given by Ferguson and Keck (70). They developed a correlation formula for the flame speed using Van Tiggelen's model for the flame speed (71). Ferguson and Keck estimated the model parameters (for propane and iso-octane) by fitting the model with experimental data in the literature. They emphasize that these parameters are estimates since they were obtained from conflicting experimental data. However, it is not clear from their discussion, over what range of  $\phi$ ,  $T_u$  and  $p_u$  the parameters were fitted. In view of this uncertainty and in view of the lack of reliable data for non-stoichiometric mixtures at high pressures and temperatures, we have used the correlation formula only for stoichiometric mixtures in our studies on the effect of  $p_u$  and  $T_u$  on the blowoff velocity.

#### 3.4 Comparison of Blowoff Velocity Correlation with Published Data

In this section, the blowoff velocity predicted by equations (6) and (8) is compared with experimental data for a range of fuel-air equivalence ratios ( $\phi$ ), inlet pressure ( $p_u$ ), inlet temperature ( $T_u$ ), flameholder characteristic dimension ( $d$ ), and Reynolds number ( $Re$ ) based on the free stream velocity, flameholder size and the state of the combustible gas stream.

##### Equivalence Ratio

The effect of varying the fuel-air ratio upon the relative blowoff velocity  $U_r$  (defined as  $U_r = U_b/U_{b,ref}$ , where  $U_{b,ref}$  is the blowoff velocity of the stoichiometric fuel-air mixture), was compared using equation (8) and the correlation for the laminar flame speed given in reference (70). Note that for purely relative calculations no specific value need be assigned to the parameter  $R_1$ ; it is merely assumed to be constant for a given flameholder-combustor combination. In Figure 4, a plot of  $U_r$  versus the fuel-air equivalence ratio  $\phi$  and experimental data taken from various sources are presented. The model correlation and experimental data are for a propane-air mixture at an inlet pressure and temperature of 1 atmosphere and 300 K respectively. Excellent agreement between the correlation and experimental data is obtained for fuel-lean equivalence ratios. For rich mixtures, there is considerable scatter in the experimental data which appear to be dependent on the experimental apparatus as well as the characteristics of the bluff body stabilizing the flame. This scatter also appears for correlations of rich laminar flame speeds and appears to be characteristic of fuel-rich combustion. The data scatter in Figure 4 implies that possibly the diffusion of active species in fuel-rich flames are being affected by the characteristic flows of each device.

## Inlet Pressure

The pressure dependence in the blowoff velocity is a result of the density term in the kinematic viscosity, and the laminar flame speed pressure dependence. The density varies directly with pressure ( $p_u$ ) so that (see equation (8)), the blowoff velocity varies as the  $(2\alpha + 1)$  power of the pressure where  $S_L \propto p_u^\alpha$ .

There are considerable discrepancies in the literature on the value of  $\alpha$ . According to Lavoie (69),  $\alpha$  has a value  $-0.2$  for stoichiometric propane-air mixtures. Metghalchi and Keck (72) experimentally determined values of  $-0.26$  and  $-0.12$  for stoichiometric mixtures of methane-air and isooctane-air respectively. But, Andrews and Bradley (68) recommend  $-0.5$  for stoichiometric methane air mixtures. It is also believed that many hydrocarbon fuels have little or no pressure dependence (73). Also, both the quenching distance and the flame thickness increase rapidly as the pressure is reduced which leads to larger errors in the measurements of the flame speed (68).

The above discussion implies that the pressure exponent of the blowoff velocity ranges from zero ( $\alpha = -0.5$ ) to one ( $\alpha = 0$ ) for hydrocarbon-air mixtures. The laminar flame speed correlation used here has a small pressure dependence ( $\alpha = -0.06$ , see reference (70)) and so the agreement between the correlation given by equation (8) and the curve  $U_b \propto p_u$  is good (see Figure 5).

In addition to the data points shown in Figure 5, DeZubay (26) concluded that the blowoff velocity varied as the  $0.95$  power of the pressure for disk flameholders. Surlock (22) found a linear pressure dependence for transverse cylindrical flameholders. Blowoff data on ramjet flameholders also indicate that the blowoff velocity varies directly with the pressure (18). However, most of this work was done at subatmospheric pressures in closed systems which are prone to pressure fluctuations. Pressure (and flow) fluctuations can cause the flame to go unstable thereby resulting in much lower blowout velocities (14, 15, 35).

The meagre high pressure experimental data that is available shows little or no pressure dependence. Longwell et al (24) found that for baffle stabilized flames, pressure changes between 1 and 3 atmospheres had little effect on the lean stability limit. In a more recent study on flames stabilized behind perforated plates, Roffe and Venkatramani (42,43) report that, increasing pressure from 5 to 30 atmospheres did not affect the lean stability limit for a reference velocity of 25 m/s.

## Inlet Temperature

The dependence of the blowoff velocity on the inlet temperature ( $T_u$ ) of the fuel-air mixture is a result of the temperature dependence of the kinematic viscosity and the laminar flame speed. The temperature dependence of the kinematic viscosity can be reasonably approximated by a power law (74). Also, for a limited range of  $T_u$ , the laminar flame speed dependence can be expressed

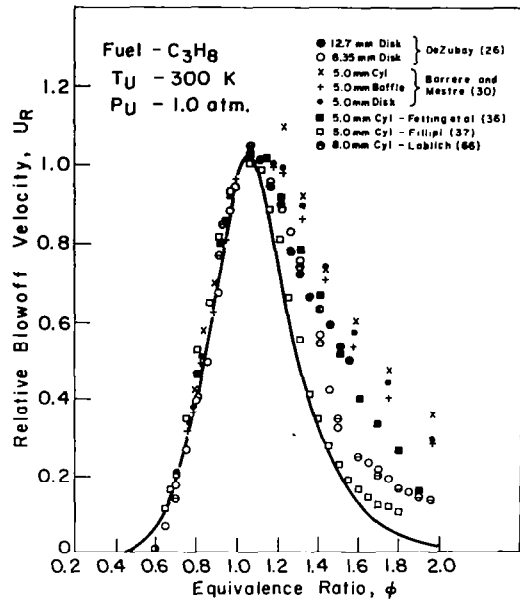


Figure 4

Relative Blowoff Velocity Versus Equivalence Ratio. Solid line represents the proposed correlation compared with published data.

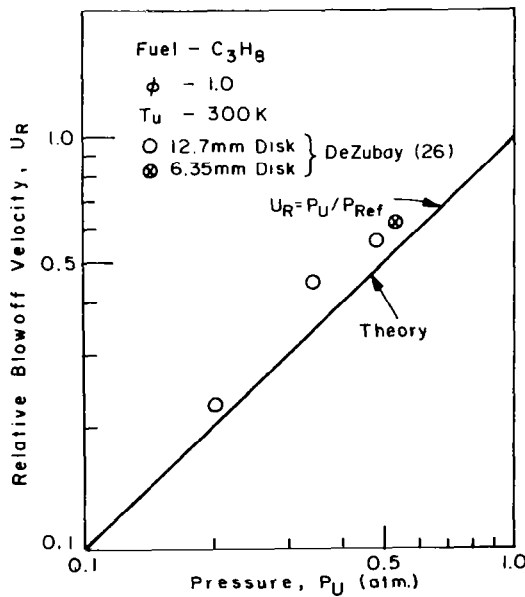


Figure 5

Relative Blowoff Velocity as a Function of Pressure for an Equivalence Ratio of 1.0 and Unburned Charge Temperature of 300 K. Line marked theory represents the results of the proposed correlation.

locally by a power law so that the conventional representation of the stability criterion ( $U_b/T_u^\beta$ ) can be obtained from equation (8). A curve of the relative blowoff velocity  $U_r (= U_b/U_b @ 300 \text{ K})$  for  $\phi = 1.0$  and  $p_u = 1 \text{ atm.}$  versus  $T_u$  derived from equation (8), is shown in Figure 6. This curve corresponds quite well with the power law  $(T_u/300 \text{ K})^{1.5}$  up to 700 K. Detailed investigations of the temperature effect on the blowoff velocity are limited to those of Haddock (27) and Mestre (31). Their investigations showed that the blowoff velocity varies as the approach stream temperature raised to the 1.2 to 1.5 power. Ramjet blowoff data correlate with the inlet air total temperature raised to the 1.5 power (18). The behaviour of the curve for  $T_u > 800 \text{ K}$  indicates that the temperature dependence may be exponential rather than a power of  $T_u$ . In other words, the temperature dependence due to the kinematic viscosity may be less important than that of the laminar flame speed. Lack of blowoff data for  $T_u > 800 \text{ K}$  prevents quantitative comparisons in this regime.

#### Flameholder Characteristic Dimension

The expression for the blowoff velocity given in equation (8) shows the blowoff velocity to be linearly related to the length  $L$  of the recirculation zone. However,  $L$  has to be related to the characteristic dimension  $d$  of the flameholder before the effect of  $d$  on the blowoff velocity can be gauged. A number of investigators have studied experimentally the effect of flameholder size, approach stream velocity and equivalence ratio of the approach stream on the length of the recirculation zone (33, 34, 38, 39). These investigations showed that the ratio  $L/d$  is constant for sufficiently high Reynolds numbers. Moreover,  $L$  was found to be practically constant over a wide range of equivalence ratios. The introduction of  $L \propto d$  into equation (8) implies that the

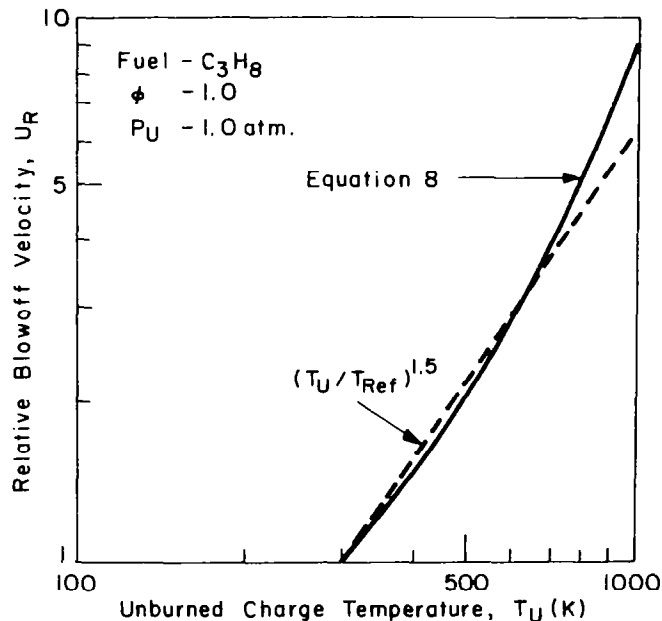


Figure 6 Relative Blowoff Velocity versus Unburned Charge Temperature for  $\phi = 1.0$  and  $P_u = 1.0 \text{ atm.}$  Solid line represents the correlation results.

blowoff velocity is related to the characteristic size of the flameholder by

$$U_b \propto S_L^2 d(1 - R_B)/\nu \quad (9)$$

where,  $R_B$  is the blockage ratio of the flameholder (see equation (7)). If  $\phi$ ,  $T_u$  and  $p_u$  are held constant for a given fuel, then equations (9) reduces to

$$U_b \propto d(1 - R_B) \quad (10)$$

For flameholders whose characteristic sizes are much smaller than the duct dimensions (i.e.  $R_B \ll 1$ ) equation (10) suggests that the blowoff velocity is linearly related to the characteristic size of the flameholder. Longwell (75) and others (see Ozawa (18)) have demonstrated this dependence. Furthermore, for  $R_B \ll 1$ , if  $T_u$ ,  $p_u$  and fuel type are held constant,  $S_L = S_L(\phi)$  only so that equation (9) reduces to

$$U_b = df(\phi) \text{ or } U_b/d = f(\phi) \quad (11)$$

for flameholders whose characteristic sizes are much smaller than the duct dimensions.

Equation (11) suggests that a stability loop is formed for a flameholder of a given shape but different characteristic sizes (with the constraint  $R_B \ll 1$ ), by plotting the equivalence ratio at blowoff against the blowoff velocity divided by the flameholder characteristic dimension. This fact has been demonstrated for various flameholder shapes (disk, cylinder, 90° cone, half-round channel and 90° V-gutter) by Mestre (31). Also, Ozawa (18) presents composites of results from various investigations plotted as  $U_b/d$  versus  $\phi$  for flameholders of various shapes and sizes. These composites clearly show that the blowoff velocity varies directly with the flameholder size.

Notice also that equation (9) predicts an optimum size for the flameholder. For example, consider a disk of diameter  $d$  located in a circular duct of diameter  $D$  (so that  $R_B = d^2/D^2$ ). Then for constant  $\phi$ ,  $T_u$ ,  $p_u$ , and fuel type, we have from equation (10)

$$U_b \propto d(1 - d^2/D^2)$$

which has a maximum for  $d = D/\sqrt{3}$  corresponding to a blockage ratio of 33 percent. Thus, increasing the characteristic size of the flameholder leads to an increase in  $U_b$ ; however, when the size of the stabilizer exceeds  $D/\sqrt{3}$  a further increase in  $d$  results in a decrease in  $U_b$ . This effect of the flameholder dimension on the blowoff velocity has been reported by Williams and Shipman (28) and by Friedman et al (44). In fact, for an annular V-gutter in a ramjet engine, Friedman et al found that the value of the blockage needed to optimize the stability characteristic of the burner was in the range 30 to 40 percent.

It would seem from the above discussion that the velocity at the edge of the flameholder ( $U_2$ , see Figure 1) is a better measure of the velocity which determines stability. For constant  $\phi$ ,  $T_u$ ,  $p_u$  and fuel type, for  $L \propto d$ , equation (6) reduces to  $U_2 \propto d$ ; at blowoff, the velocity in the plane of the flameholder is linearly related to the size of the flameholder. This fact has been experimentally demonstrated by Longwell et al (24).

#### Reynolds Number

The functional dependence of the blowoff velocity on the Reynolds number is deduced by rearranging equations (6) and (8) to yield

$$U_2 = R_\tau S_L (U_2 L / \nu)^{1/2} \quad (12)$$

and

$$U_b = R_1 S_L (U_b L / \nu)^{1/2} \quad (13)$$

These equations state that the blowoff velocity varies as the square root of the Reynolds number for a given  $\phi$ ,  $T_u$ ,  $p_u$  and fuel type. Zukoski and Marble (32) have shown that  $U_b$  varies approximately as the square root of the Reynolds number ( $U_b d / \nu$ ). Their results are shown in Figure 7 along with the dependence for  $U_b$  given in equation (13) (with the assumption  $L \propto d$ ). The agreement between the correlation and the experimental data is exceptionally good.

Figure 8 shows curves of  $U_b / S_L$  against  $U_b d / \nu$  taken from various sources. We notice that all the data fall on straight lines of slope 1/2, but they have different multiplying constants  $R_1$ . This figure justifies the assertion that although  $R_1$  can vary from one flameholder-combustor configuration to another, it is constant for fixed flameholder and combustor geometries. Notice, however, that  $R_1$  is always of order unity.

Although the value of  $R_1$  is not a universal constant, the value of  $R_\tau$  should not change significantly from one flameholder-combustor combination to another. A real test of the model is therefore a plot of  $U_2 / S_L$  against  $U_2 L / \nu$  (from equation (12)). Ideally, all the data points should follow a single straight line of slope 1/2. Furthermore, the constant  $R_\tau$  evaluated from this line should be of order unity. This has been done with most of the data\* in Figure 8 and is presented in Figure 9. Estimates of  $L/d$  were made from values in the literature and  $U_2$  was calculated using equation (7). The estimates made for  $L/d$  and the sources are given in Table 1. Notice that, after Winterfeld (38), values of  $L/d$  for cylindrical flameholders increase with the stoichiometric blow-off velocity (see Figure 6 in reference (18)).

---

\* Some of the data had to be rejected as insufficient information has been given about the geometry of the flameholder or the combustor;  $U_2$  could not, therefore, be calculated.

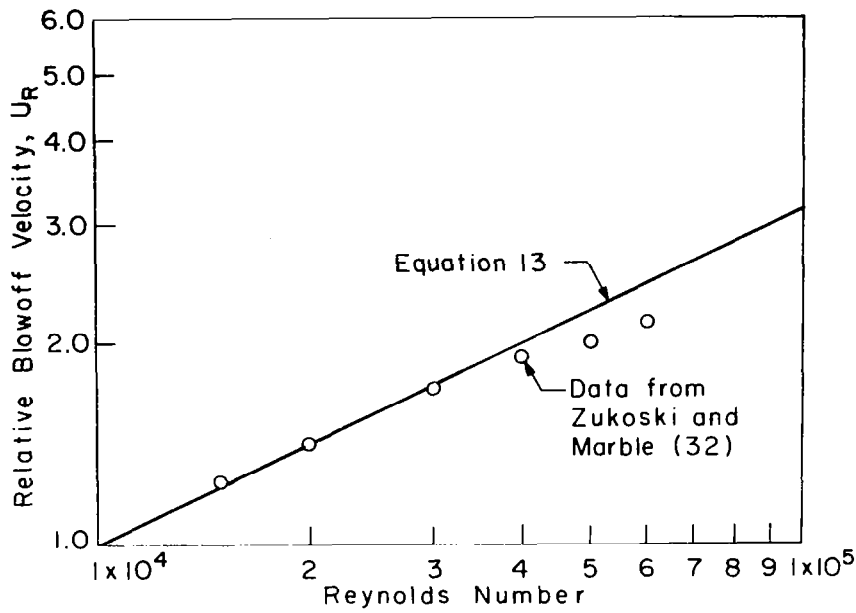


Figure 7 Relative Blowoff Velocity Versus Reynolds Number. Solid line is the correlation given by equation 13 and is compared to data of Zukoski and Marble (32).

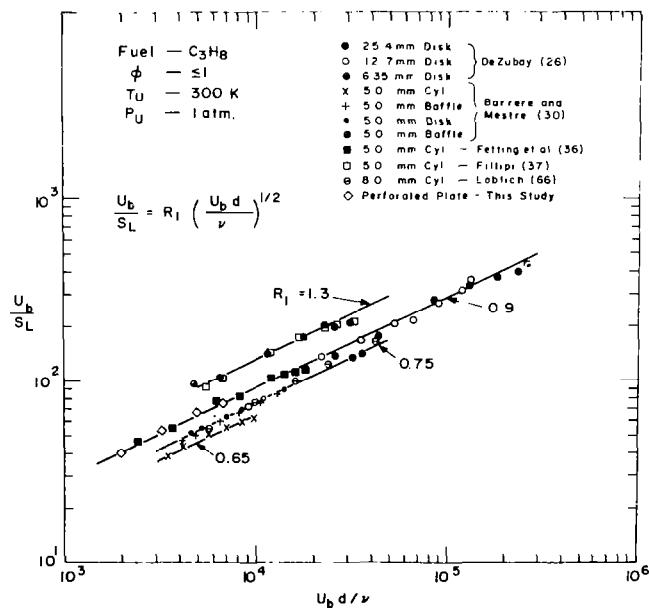


Figure 8 Plots of Blowoff Velocity ( $U_b$ )/Laminar Flame Speed Against Reynolds Number Based on  $U_b$ , the Flameholder Characteristic Dimension and the State of the Unburned Charge.

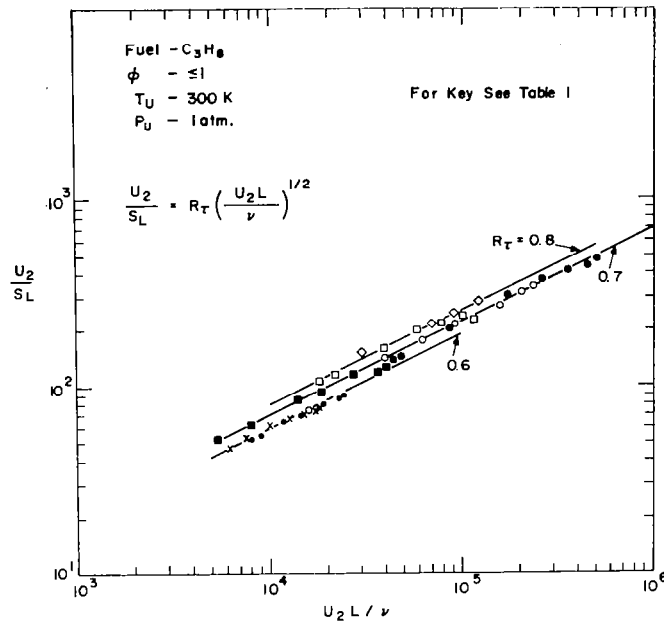


Figure 9 Plots of Velocity, at Blowoff, in Plane of Maximum Flameholder Blockage ( $U_2$ )/Laminar Flame Speed Versus Reynolds Number Based on  $U_2$ , the Recirculation Zone Length and the State of the Unburned Charge.

We notice (Figure 9) that although a single straight line does not collapse all the data, the scatter in the value of  $R_\tau$  is small. This scatter could be attributed to uncertainties in the value of  $L/d$ . This figure provides justification for the use of  $U_2$  (and not  $U_b$ ) as the measure of the velocity which determines stability. Figure 9 also shows that the length of the recirculation zone is a more fundamental indicator of the stability characteristics of a flameholder than its characteristic size.



Table 1  
 Estimates for Lengths of Recirculation  
 Zones behind Flame Stabilizers used for  
 Figure 9.

Symbol From Fig. 9	Source	Flameholder		Stoichiometric Blowoff Velocity (m/s)	L/d	Source
		Shape	Size (mm)			
⊙	26	disk	12.7	154	1.7	24
⊕	26	disk	6.35	64	1.7	24
●	26	disk	25.4	- -	1.7	24
•	30	disk	5.0	41	1.7	24
×	30	cylinder	5.0	35	1.5	18,38
■	36	cylinder	5.0	53	2.0	18,38
□	37	cylinder	5.0	98	3.0	18,38
◇	this study	perforated plate	9.7*	- -	4.7	86

\* equivalent characteristic size

#### 4 A STOCHASTIC MIXING MODEL FOR MODELLING FLAME IGNITION AND BLOWOUT

In this section, the model developed for studying the effects of mixture nonuniformity on the lean ignition and blowout limits of turbulent flames is described. In a typical combustor, the fuel and air enter the primary zone separately. As the fuel and air mix, they form turbulent "eddies" or pockets of combustible mixture with a distribution in fuel-air ratio about the mean primary value. This distribution will change with time as these eddies mix with each other, through the action of turbulence and molecular diffusion.

The primary zone unmixedness (or nonuniformity) can be quantified as follows. Since the fuel and air are not uniformly mixed, different gas eddies will have different fuel fractions during their residence time in the combustor primary zone. The use of fuel fraction  $F$  (fuel mass divided by total mass) in a mass-based distribution function simplifies the mathematics, compared to using fuel-air ratio or equivalence ratio. Assuming a Gaussian distribution function for the fuel fraction about the mean fuel fraction  $\bar{F}$ ,

$$f(F) = (1/2\pi\sigma^2)^{1/2} \exp[-(F - \bar{F})^2 / 2\sigma^2] \quad (14)$$

where  $\sigma$  is the standard deviation of the distribution, then the fraction by mass of the burned gas with fuel fraction between  $F$  and  $F + dF$  is  $f(F)dF$ . An unmixedness parameter

$$s = \sigma / \bar{F} \quad (15)$$

can be used as a measure of the mixture nonuniformity. A value of  $s = 0$  corresponds to complete premixing of the fuel and air.

To investigate the effects of a primary zone nonuniformity on the lean ignition limit, a statistical mixing model has been developed. This model is described in section 4.1 and the calculation procedures for determining the lean ignition and blowout limits are detailed in section 4.2. The effects of inlet pressure, temperature and mixture velocity on the lean ignition and blowout limits of a premixed fuel-air system (i.e.  $s = 0$ ) are explored in section 4.3. We conclude section 4.3 with a study on the effects of mixture nonuniformity (by varying  $s$ ) on the lean ignition limit.

##### 4.1 A Statistical Model with Monte Carlo Mixing

A statistical model of following a chemical reaction through a mixing process was described by Corrsin (76) and adapted by Flagan and Appleton (13) who applied a plug flow Monte Carlo coalescence/dispersion model to a practical combustor. The agreement between their model predictions of  $\text{NO}_x$  and experimental values was excellent. Mikus et al (11) have used this model to study the effects of mixture nonuniformity on  $\text{NO}_x$  formation rates in gas turbine combustors. The ease with which mixture nonuniformities can be incorporated into the computational scheme makes the stochastic Monte Carlo coalescence/dis-

persion model particularly attractive for this study. A brief description of the model is given below: Pratt (77,78) gives a good review of this and other Monte Carlo coalescence/dispersion models.

In this model, the region immediately downstream of the flameholder - where the flow field must include recirculation zones for flame stability - is characterized as a partially stirred (or macromixed) reactor. In this study the flameholder was a perforated plate. The composition of the reactor at any time is described by a statistical ensemble of (N) equal mass fluid elements which have a distribution of thermodynamic states. Each element is assumed sufficiently small that its state may be assumed uniform throughout its volume. At any point in time, each element has its own local fuel fraction. The number of elements (N) should be large enough to characterize the distribution of fuel fractions and thermodynamic states. This number was between 100 and 1000 for the calculations presented here.

The ensemble of fluid elements experiences mixing interactions which represent the mixing process. These interactions occur at time intervals  $\Delta t_m$  given by

$$\Delta t_m = 1/\beta N \quad (16)$$

where,  $\beta$  is the mixing frequency. Each mixing interaction is computed as follows: (a) A pseudorandom number generator is used to identify two different fluid elements, (b) The properties of these two elements are evaluated at the time of mixing, (c) The two elements are allowed to mix completely and reach a mean composition and temperature depending on their state of burnedness. Both elements are assigned a new fuel fraction equal to the average of the two prior to mixing and (d) The elements then separate, and the chemical reactions proceed within each element (in accordance with the appropriate rate equations) depending on the new composition and temperature.

The mixing frequency  $\beta$  is empirically determined. From experimental studies on air-assist atomizers with gaseous fuels, Komiyama (79) has shown that the mixing frequency in the primary combustion region is given by

$$\beta = c_\beta (P_j/ML^2)^{1/3} \quad (17)$$

where  $P_j$  is the input flow power, M is the mass of the fluid in which this power is dissipated, L is the length over which the mixing takes place and  $c_\beta$  is a constant of order unity. The value of  $c_\beta$  represents the efficiency of transfer of kinetic energy to turbulent flow. In this study,  $\beta$  was assumed to be constant within the reactor and the length L was assumed equal to the length of the recirculation zone downstream of the flameholder.

In a continuous flow combustor, unburnt fuel-air mixture flows into the primary zone and a mixture of unburnt, burning and burnt gases flows out of this zone. This transport of mass into and out of the reactor is simulated by element additions and removals. These "flux events" occur at time intervals  $\Delta t_r$  given by

$$\Delta t_r = \tau_r / N \quad (18)$$

where  $\tau_r$  is the average residence time for the reactor

$$\tau_r = V / (\dot{m} \bar{v}) \quad (19)$$

where  $V$  is the volume of the reactor,  $\dot{m}$  is the mass flow rate through the reactor, and  $\bar{v}$  is the mean specific volume within the reactor. Equation (19) can be rewritten in terms of the length  $L$  of the reactor, and the approach flow velocity  $U$  as

$$\tau_r = c_\tau L/U \quad (20)$$

where  $c_\tau$  is a constant which depends on the flameholder. By definition,  $c_\tau = 1$  for isothermal flow; however, it has to be estimated for hot flow.

To simulate the random nature of the flow within the reactor, at time intervals of  $\Delta t_r$ , an element is randomly chosen to be removed from the reactor. This element is then replaced by an unburnt element at the inlet conditions.

The choice of which event, a mixing interaction or the removal and addition of elements is determined by a time check. If the time for the next mix is less than the time for the next flux, a mixing interaction occurs; otherwise a flux event occurs. The mix (or flux) time is then updated for the next event. At any time, the mean composition and other mean properties of the ensemble may be evaluated by integrating the appropriate chemical rate equation up to that time and by taking an average over the  $N$  fluid elements.

The following kinetic model was used. The combustion of hydrocarbon fuels with air is known to be a complex process. Uncertainties exist in both the mechanisms and rates for high temperature oxidation of these fuels and the resulting intermediate species. Any detailed mechanism describing the oxidation of higher hydrocarbons results in a large number of species and reaction steps. The complexity involved in the use of detailed reaction mechanisms leads to excessive computer costs. An overall rate equation was used to describe the chemical kinetics of the fuel; this is adequate for the applications presented here since we are primarily interested in the rate of disappearance of the fuel due to combustion.

Significant discrepancies exist in the reaction rates for higher hydrocarbons. For example, Schefer and Sawyer (80), report a difference of two orders of magnitude between predicted propane disappearance rates (calculated using an overall approximation for propane oxidation) and those obtained experimentally. In view of these uncertainties it was decided to study the trends (in the lean ignition and blowout limits) predicted by the stochastic mixing model using a relatively simple fuel, methane, whose oxidation process has

been extensively studied. An overall rate expression due to Dryer and Glassman (81, 82) was used for the methane oxidation:

$$\frac{d}{dt} [\text{CH}_4] = -10^{13.2} \exp(-48400/RT) [\text{CH}_4]^{0.7} [\text{O}_2]^{0.8} \text{ mole/cm}^3\text{s} \quad (21)$$

The model assumes that the products of combustion are solely carbon dioxide, water, nitrogen which acts as a diluent and (possibly) oxygen.

#### 4.2 Computational Procedures

The computational procedures used for predicting the lean ignition and blowout limits were essentially the same. The sequence for determining these limits is as follows:

- 1) For given values of the mean equivalence ratio ( $\bar{\phi}$ ) and unmixedness parameter ( $s$ ) in the primary zone the fuel fraction distribution is calculated via equations (14) and (15). For the perfectly mixed case ( $s = 0$ ) all elements have the same fuel fraction.
- 2) For the given inlet conditions ( $T_u, P$ ) the unburned gas state is computed according to equation given by Hires et al (83) together with appropriate polynomials to describe the fuel's enthalpy (84). These calculations are done for a wide range of fuel fractions and the results stored in a table. Each element is assigned unburnt properties depending on its fuel fraction; these properties are obtained by interpolation from the table of values.
- 3) Burnt properties are assigned to the elements in the same way. Assuming an adiabatic constant pressure combustion process, the burnt mixture properties are calculated using the model described by Martin and Heywood (85).
- 4) To model flame ignition, the ensemble of elements is initialized at time  $t = 0$  by stating that all the elements are unburnt. Their properties are  $B$  (= burnt fraction) = 0,  $T = T_u$ ,  $c_p = c_{p,u}$  corresponding to the element's fuel fraction, etc. The sparking process is replaced by stipulating that at time  $t = 0$ , a few ( $n$ ,  $n/N \ll 1$ ) of these elements are fully burnt so that their properties become  $B = 1$ ,  $T = T_{ad}$  corresponding to the element's fuel fraction, etc. The burnt fraction of the ensemble at  $t = 0$  is therefore  $n/N (\ll 1)$ . To model blowout, the ensemble of fluid elements is initialized at time  $t = 0$  by assuming that most, or all,  $n_b$  of the elements ( $1 - n_b/N \ll 1$ ) are fully burnt at this time.
- 5) The mixing process and material flow through the primary zone are simulated in the manner described in section 4.1.
- 6) Elements which are partially burnt ( $0 < B < 1$ ) are assumed to comprise a mixture of gases. From an overall viewpoint, an average specific heat and a (uniform) temperature are therefore easily specified.
- 7) At any time  $t$ , the mean properties of the ensemble are evaluated by numerically integrating the chemical rate equation for each element (provided its burnt fraction  $> 0$ ) up to that time and by taking an average over the  $N$  fluid elements.

In the manner described above, the properties of the ensemble are allowed to evolve with time.

The 'ignition limit' was determined as follows. For a given set of initial conditions ( $T_u, P, U, s$ ) the computer program is run for various equivalence ratios ( $\phi$ ). Figure 10 presents a series of ensemble burnt fraction versus nondimensional time ( $t^* = t/\tau_r$ ) for inlet conditions of  $T_u = 500$  K,  $P = 1$  atm,  $U = 25$  m/s and  $s = 0$ . We note that the rate of burning increases with the equivalence ratio. This is due to an increase in the temperature of the burned products as there is more fuel per unit mass of mixture. This increase in temperature results in an increase in the rate of burn up because the chemical kinetics are very temperature sensitive. Also, notice that for  $\phi = 0.75$  and  $0.76$  the ensemble burned fraction after one residence time is little changed from its initial value: for  $\phi = 0.76$ , it is higher. The lean ignition limit therefore lies between these two values. We have designated the higher value as the lean ignition limit: it may therefore be thought of as the leanest mixture for which ignition is possible. Notice that this definition is consistent with the experimental procedure for determining the lean ignition limit (see section 5.5.1). For this example ( $T_u = 500$  K,  $P = 1$  atm.,  $U = 25$  m/s,  $s = 0$ ) the model has predicted a lean ignition limit of  $0.76$ . We have restricted the computation time to one residence time because a requirement for flame stabilization is that the residence time be longer than the characteristic ignition time (10). Moreover, computations carried out for much longer times showed essentially no change in the lean ignition limit.

To determine the lean blowout limit, the ensemble of fluid elements was initialized as described previously, and the ensemble properties were allowed to evolve with time. Blowout is characterized by the burnt fraction continuously decreasing with time to approach zero. Figure 11 presents a series of ensemble burnt fraction versus nondimensional time ( $t^* = t/\tau_r$ ) for inlet conditions of  $T_u = 500$  K,  $P = 1$  atm.,  $U = 25$  m/s and  $s = 0$ . We notice that for  $\phi \leq 0.65$ , the ensemble burnt fraction continuously decreases with time to approach zero thereby indicating flame blowout. The fluctuations in the curve are a result of the random feature of the stochastic model. Figure 12 shows a plot of the ensemble burnt fraction at steady state as a function of equivalence ratio for  $T_u = 500$  K,  $P = 1$  atm.,  $U = 25$  m/s and  $s = 0$ . The burnt fraction shows little change with  $\phi$  until at some value of  $\phi$ ,  $B$  drops rapidly. This is precisely the behavior observed near blowout (see section 5.5.2 and Figure 21). The model has predicted a blowout equivalence ratio limit of  $0.65$  for the inlet conditions given above.

#### 4.3 Results and Discussion

The statistical model predictions are presented in this subsection. We first study the predicted trends for the lean ignition and blowout limits of uniform mixtures, and compare them with experimental observations and data. Then, the effect of mixture nonuniformity on the lean ignition limit is examined.

##### 4.3.1 Parametric Studies for Uniform Mixtures

The procedures outlined in section 4.2 were used to determine the lean

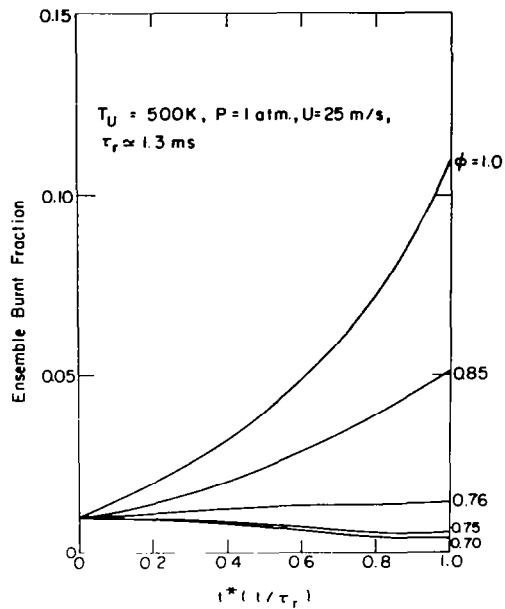


Figure 10 Ensemble Burnt Fraction Versus  $t^*$  for Various Equivalence Ratios for  $T_U = 500\text{ K}$ ,  $P = 1\text{ atm}$ ,  $U = 25\text{ m/s}$ ,  $s = 0$ .

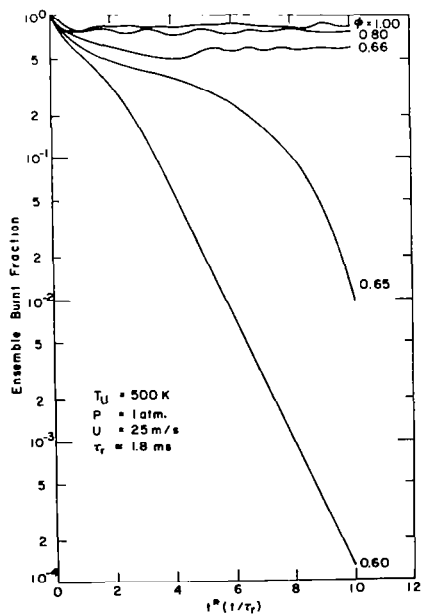


Figure 11 Ensemble Burnt Fraction Versus  $t^*$  for Various Equivalence Ratios for  $T_U = 500\text{ K}$ ,  $P = 1\text{ atm}$ ,  $U = 25\text{ m/s}$ ,  $s = 0$ .

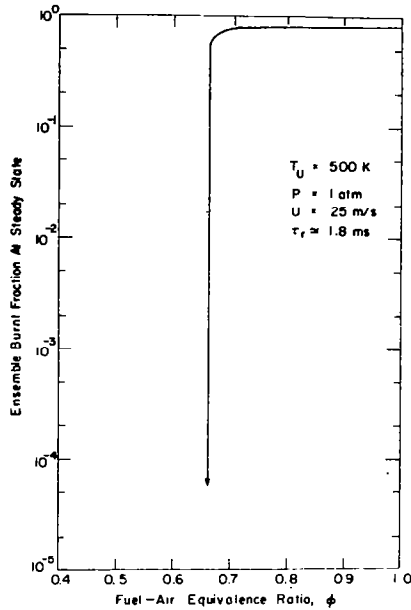


Figure 12 Ensemble Burnt Fraction, at Steady State, Versus Equivalence Ratio for  $T_u = 500 \text{ K}$ ,  $P = 1 \text{ atm.}$ ,  $U = 25 \text{ m/s}$ ,  $s = 0$ .

ignition and blowout limits of a premixed methane/air mixture under various inlet conditions. This problem was chosen so that trends of the model predictions could be assessed by comparisons with experimental observations. The combustor and flameholder modelled in this study are described in Section 5.1. The lengths  $L$  of the recirculation zone (and hence, the reactor) in both isothermal and hot flows were obtained by visualization techniques as described by Radhakrishnan (86). The mixing frequency was calculated using equation (17) with  $c_\beta = 1$ . The constant,  $c_\tau$ , for hot flow was estimated as follows. For the flameholder and combustor modelled in this study, Anderson (6) showed that a residence time of 2 ms (for  $U = 25 \text{ m/s}$ ) gave good agreement between measured and calculated (using a well-stirred-reactor model) nitric oxide levels. Using these values of  $\tau_r$  and  $U$  and the value of  $L$  of 46 mm (86), one obtains from equation (20)  $c_\tau = 1.09$ . For convenience a value of  $c_\tau = 1.0$  was used to compute  $\tau_r$ .

The parameters chosen for this study and their effects on the lean ignition and blowout limits are discussed below:

(i) Inlet Temperature: Increases in inlet temperature lead to higher temperature burned products and hence increased burning rates. These faster burning rates imply that, at constant inlet velocity, the lean ignition and blowout limits should decrease with increasing inlet temperature. This behavior is displayed by the curves presented in Figure 13. Figure 14 shows a series of lean ignition and blowout curves against reference velocity for different inlet temperatures.



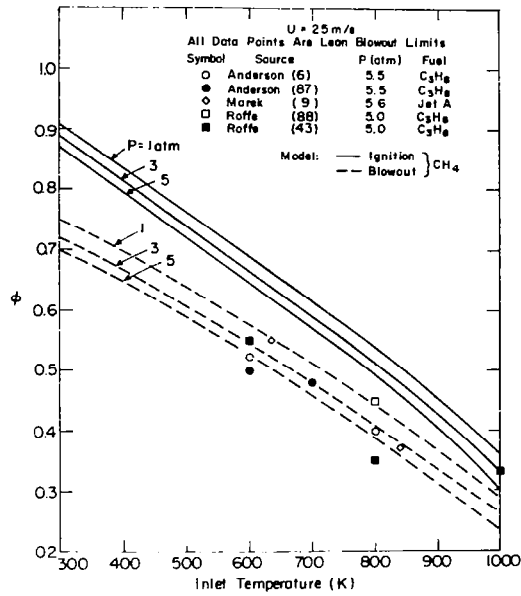


Figure 13

Variations of Predicted Lean Ignition and Blowout Limits of Uniform Mixtures with Inlet Temperature for Different Pressures.

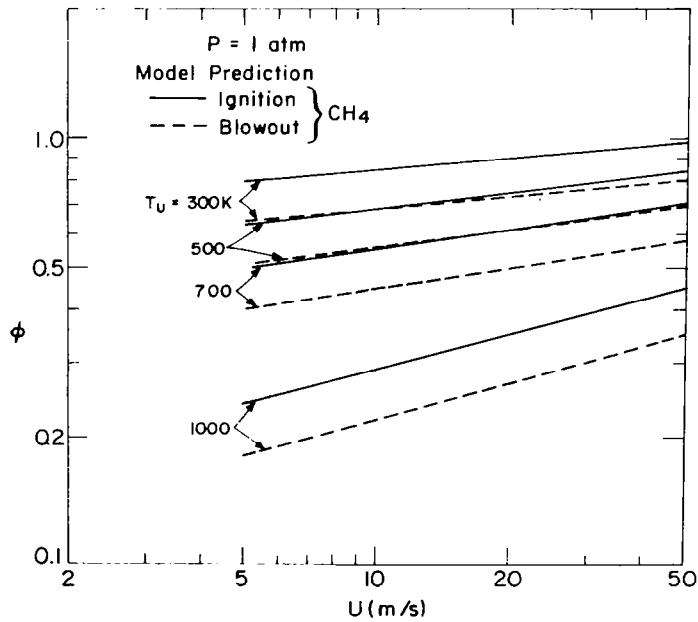


Figure 14

Variations of Predicted Lean Ignition and Blowout Limits of Uniform Mixtures with Reference Velocity for Different Inlet Temperatures.

It is apparent that for a given fuel-air equivalence ratio, increases in inlet temperature lead to higher ignition and blowout velocities. The fact that blowout velocities increase with inlet temperature has been experimentally established for laboratory scale burners and full scale engine combustors (18). Also shown on Figure 13 are some data points taken from the literature; these experimental values were obtained for apparatus very similar to the one modelled here. The agreement between the predicted and measured blowout limits is good.

(ii) Inlet Pressure: The dependence of the lean ignition and blowout limits on the inlet pressure is also shown in Figure 13. We notice that neither the lean ignition limit nor the lean blowout limit has a strong dependence on the inlet pressure. This is consistent with the known fact that increasing the inlet pressure above 1 atmosphere has a small effect on the lean flammability limit of a methane/air mixture (89). From experiments carried out with propane/air mixtures in a constant volume bomb, Bolt and Harrington (90) concluded that inlet pressures between 1.7 and 12.2 atmospheres had no noticeable effect on the lean ignition limit for either stagnant or moving mixtures. Longwell et al (24) have experimentally demonstrated that for pressures between 1 and 3 atmospheres, the pressure has a weak influence on the lean blowout limit. In a more recent study on an apparatus similar to the one modelled here, Roffe and Venkatramani (42, 43) found no pressure dependence of the blowoff velocity, for pressures between 5 and 30 atmospheres.

(iii) Reference Velocity: The variations of the lean ignition and blowout limits with mixture velocity are shown in Figure 14. We see that with increased velocity, the lean limits are richer. This requirement of richer mixtures for successful ignition at higher velocities has been experimentally demonstrated by Bolt and Harrington (90) and by Ballal and Lefebvre (91). The fact that the blowoff velocities increase with the richness of the (lean) mixture has been observed by several workers in the field (see reference 18 for details).

#### 4.3.2 Effect of Mixture Nonuniformity on the Lean Ignition Limit

The effect of mixture nonuniformity on the lean ignition limit was studied using the computational procedure outlined in section 4.2. To account for the nonuniformities in the fuel-air ratio in the incoming unburnt fuel-air mixture, the distribution given by equation 14 was used together with the definition of the unmixedness parameter ( $s$ ) given by equation 15. Figure 15 shows the effect of increasing  $s$  (i.e. increasing mixture nonuniformity) on the lean ignition limit for  $T_u = 500$  K,  $P = 1$  atm., and  $U = 10$  m/s. We see that with increasing mixture nonuniformity, the lean ignition limit becomes leaner. The value of  $s$  in a typical conventional combustor primary zone is about 0.5 (11). For this value of  $s$ , the lean ignition limit is  $\phi \approx 0.50$  compared to 0.69 for the uniform case. In other words, the fuel flow rate required for successful ignition in a typical combustor is about 28 percent less than that for a premixed burner. Lack of experimental data prevents quantitative comparisons with these predictions; however, we notice that the behavior of the lean ignition limit with  $s$  is as expected. It asymptotically approaches the value of the uniform case as  $s \rightarrow 0$ . Also, notice the change in the curvature at about  $s = 0.2$ ; this sug-

gests that as  $s$  is increased further ( the mixture becomes less uniform ) the lean ignition limit will reach an asymptotic value.

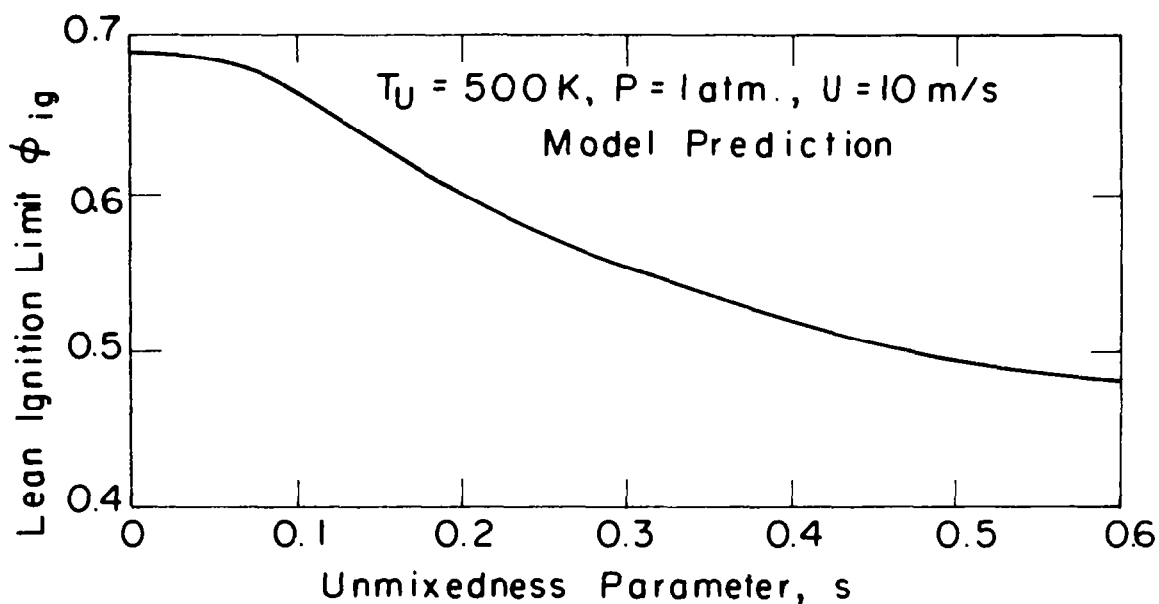


Figure 15 Variation of Predicted Lean Ignition Limit with Mixture Nonuniformity.

## 5 EXPERIMENTAL APPARATUS AND PROCEDURES

### 5.1 Experimental Hardware

The experimental work was carried out on a constant cross-sectional area tubular combustor. The experimental facility was designed to generate data on lean ignition and blowout limits and  $\text{NO}_x$  formation in fully and partially pre-mixed fuel-air mixtures. Figure 16 shows a schematic layout of the complete assembly. Air from the main laboratory compressor flows into the electrically operated pre-heater. The air heater is an 85 kW open wire duct heater that can heat the air to a temperature of about 750 K.

The preheated air flows into the fuel-air premixing section, details of which are shown in Figure 17. The premixing section consisted of modules of 0.1 m diameter stainless steel pipes of different lengths. This arrangement enabled the premixing length -- defined as the distance from the fuel injector location to the flameholder -- to be varied from a minimum of 0.33 m to a maximum of 2.50 m. This variation (of the premixing length) was achieved by re-location of the fuel injector. The whole premixing section was insulated to minimize heat loss.

Located at the upstream end of the premixing section were a fine stainless steel mesh (pore size ~ 150  $\mu\text{m}$ ), and a ceramic honeycomb (square cells of side 1 mm) about 0.1 m long and having an open area of 54 percent of the duct cross-sectional area. The mesh and the honeycomb served three purposes: (i) they reduced the nonuniformities in the velocity profile generated in the elbows downstream of the pre-heater; hot wire anemometer measurements taken immediately upstream of the flameholder location (with the flameholder removed) showed the velocity profile to be uniform to within about 10 percent; (ii) they helped damp out the pressure fluctuations present in the air supply line; and (iii) the mesh and the honeycomb were calibrated against a standard square edged ASME orifice to serve as air flow rate metering devices downstream of the preheater, to correct for preheater leakage.

Although the facility had been designed to handle both liquid and gaseous fuels, all the experimental work was done with commercial grade gaseous propane. The use of a gaseous fuel avoids the problem of prevaporization (especially for operation at room temperature). The fuel injector used in this study is shown in Figure 18. The injector was made by welding two 6.35 mm diameter stainless steel tubes to form a crucifix. Holes of diameter 0.63 mm spaced 3.1 mm apart were then drilled on the tubes. The fuel injector could be mounted to provide either streamwise or contrastream injection. However, all the experimental work was done with streamwise injection. The fuel injector design was chosen for two reasons: (i) to disperse the fuel across the duct cross-section to avoid large scale fuel distribution nonuniformities ; and (ii) to minimize flow blockage due to the injector, and hence the disturbance caused by it to the air stream.

The water cooled flameholder (Figure 19) was made by locating 64 stainless

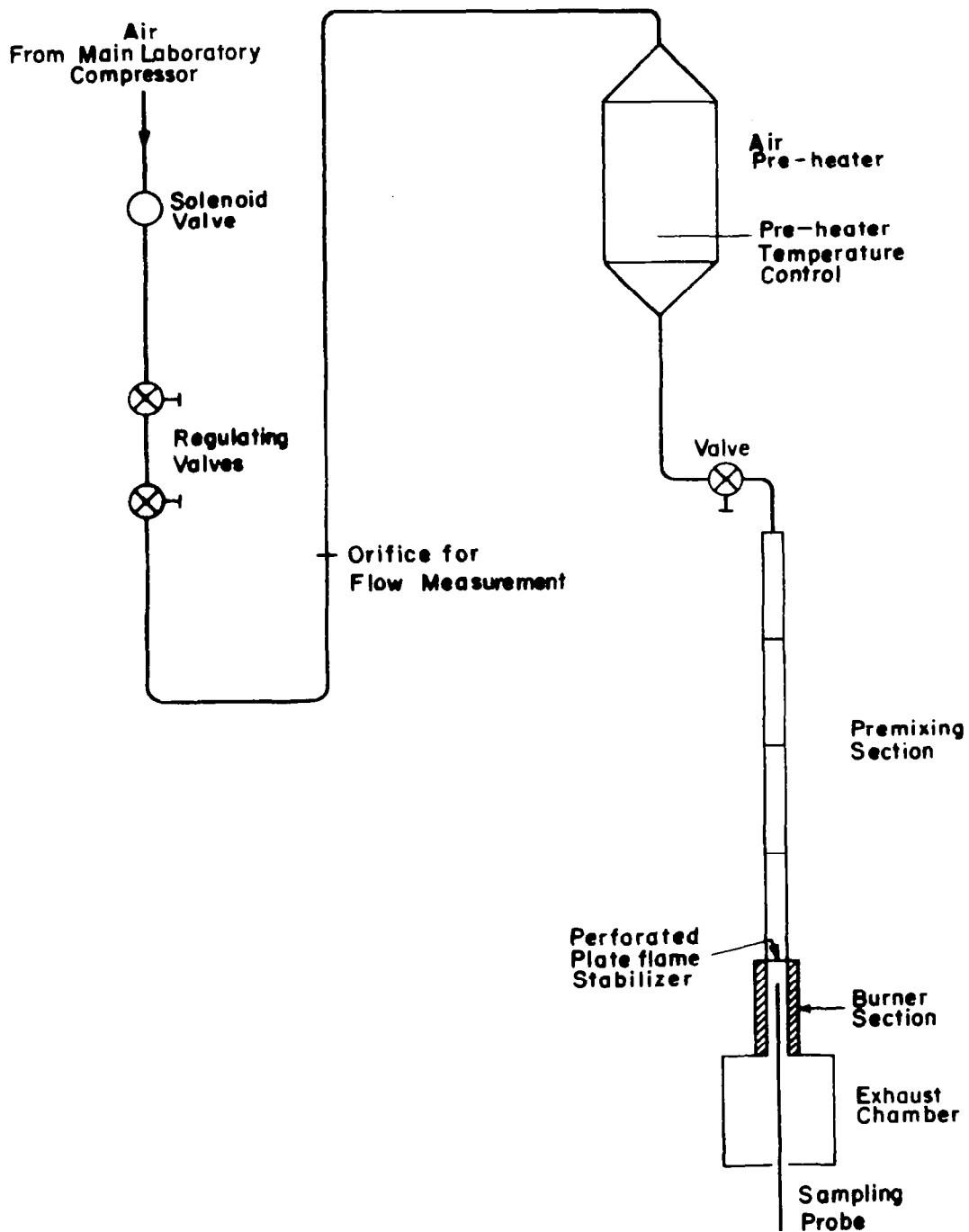


Figure 16 Schematic of Experimental Apparatus.

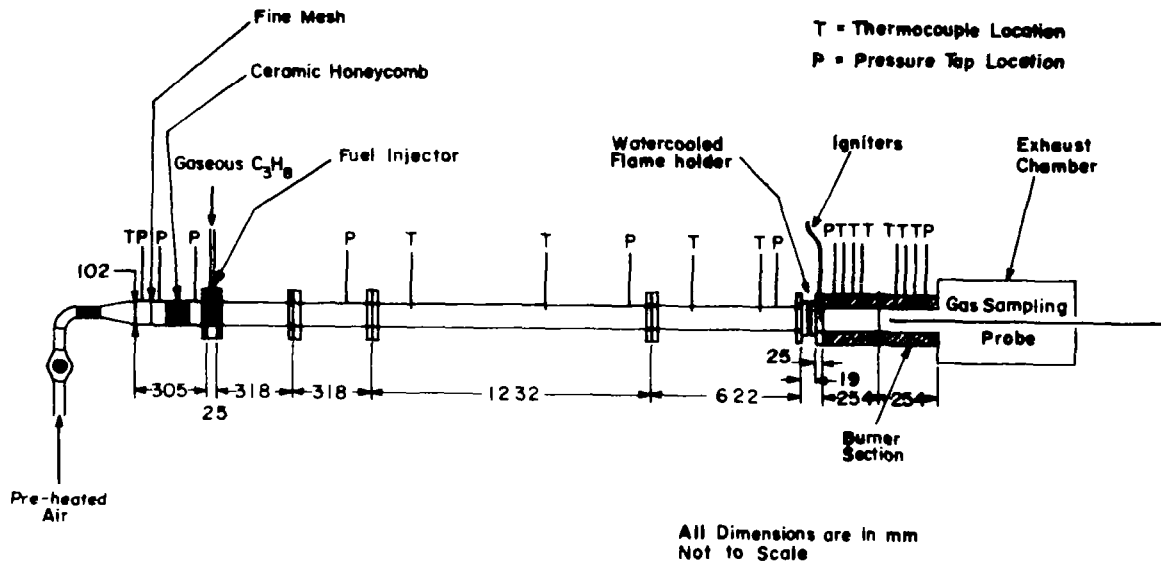


Figure 17 Fuel-Air Mixing Section Layout

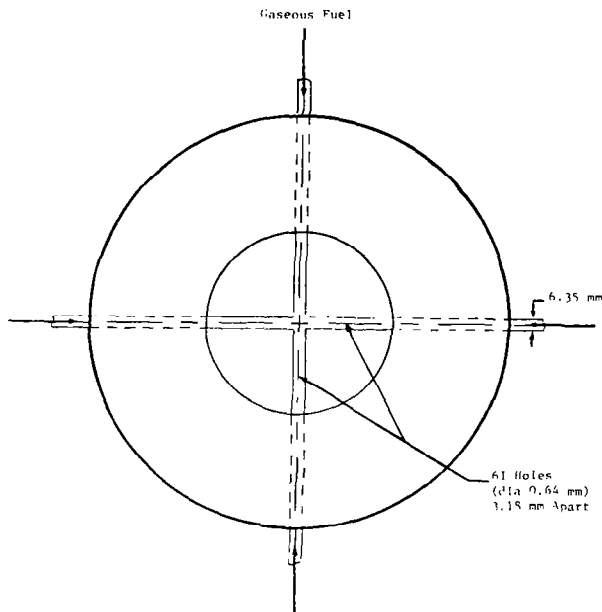


Figure 18 Gaseous Fuel Injector.

steel tubes between two 6.35 mm thick stainless steel plates. The tubes were manually expanded to an inside diameter of 6.4 mm. This arrangement resulted in an open area of 24 percent of the inlet duct cross-sectional area. The pressure drop across the flameholder ranged from 0.2 to 2 percent of the upstream pressure depending on inlet conditions.

The burner section (Figure 20) was 0.1 m in diameter (the same as the inlet duct) and 0.53 m long. The burner was lined with refractory material (to an outside diameter of 0.2 m) to minimize heat loss. A pair of standard oil burner electrodes were located in a stainless steel flange 25 mm thick immediately downstream of the flameholder. The spark gap, the size of the electrode wires and the location of the spark with respect to the flameholder could be independently varied. The combustion products were cooled in the exhaust chamber by water sprays. The mixture of combustion products and water exhausted into the building exhaust trench.

A water-cooled stainless steel probe (Figure 20) was used to sample the exhaust gases. The single point probe was 6 mm outside diameter for the first 0.23 m; it then tapered gradually to an outside diameter of 14 mm. The center sampling tube was 5 mm in diameter. The probe could be traversed in all 3 directions. It is well known that metal probes can cause a catalytic reduction of the nitric oxide by carbon monoxide. However, Halstead and Munro (92) found that for equivalence ratios less than unity, there was virtually no reduction in NO concentration by this mechanism.

## 5.2 Gas Analysis Equipment

The gas samples drawn through the probe were pulled through a length of unheated plastic tubing, then through a heated line into a diaphragm pump, then through an ice-bath moisture trap followed by desiccant tubes (except for total hydrocarbons sample) and into the continuous reading instruments. These instruments were: a Scott Model 215 Heated Total Hydrocarbon Analyzer for total hydrocarbons, standardized with methane gas; a Scott Model 150 paramagnetic analyzer for oxygen; a Beckman Model 315A NDIR analyzer for carbon dioxide; Beckman Models 315A NDIR and 864 NDIR analyzers for carbon monoxide; and a Thermo-Electron Model 10A chemiluminescent analyzer for oxides of nitrogen.

## 5.3 Instrumentation

The air flow rate was measured by means of a standard square-edged ASME orifice and the calibrated mesh and honeycomb. The pressure upstream of the orifice and the pressure drop across it were measured with mercury manometers; the pressures upstream of the mesh and honeycomb and the pressure drops across them were measured with water manometers. The fuel pressure and temperature downstream of the rotometers were measured by pressure test gauges and chromel-alumel thermocouples respectively. Fine metering valves were used to regulate the fuel flow rate.

The fuel-air mixture temperature immediately upstream of the flameholder was measured with a single chromel-alumel thermocouple inserted to a depth of

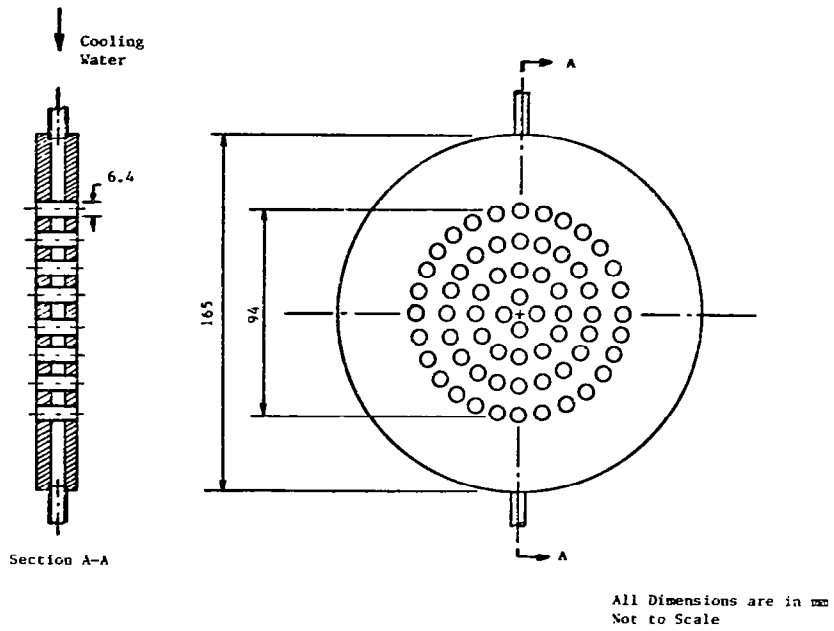


Figure 19 Flameholder.

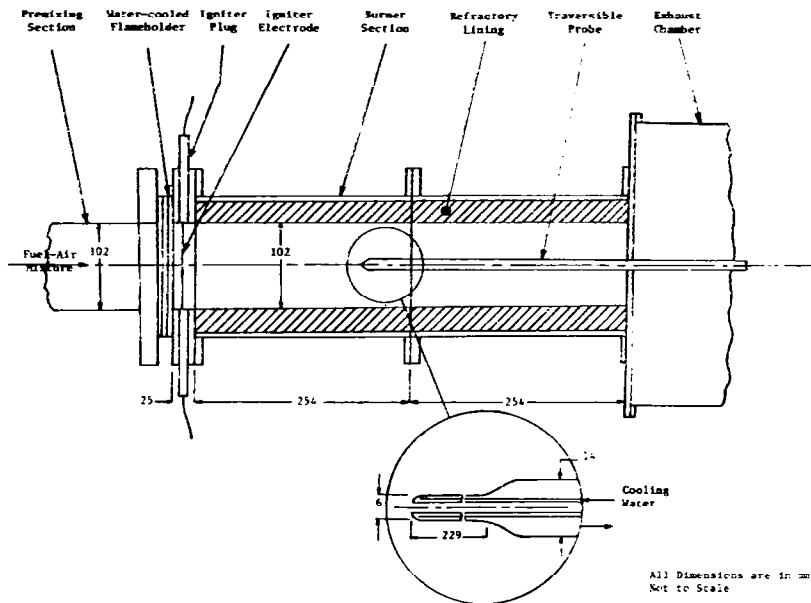


Figure 20 Burner and Component Equipment.



about 20 mm from the duct wall. The pressures immediately upstream and downstream of the flameholder were measured by water manometers, as was the pressure at the downstream end of the burner.

The burner wall temperatures were measured with chromel-alumel thermocouples as were the water temperatures into and out of the flameholder. The flameholder and gas analysis probe cooling water flow rates were measured with rotometers. When the water temperature at the probe exit was needed, it was measured with a mercury-in-glass thermometer.

#### 5.4 Safety Features

Although the technique of premixing and prevaporizing shows potential for low  $\text{NO}_x$ , experiments with premixed flames present significant practical problems. One is the possibility of flame propagation upstream of the flameholder to the fuel injector (flashback). Another is the possibility of chemical reactions in the premixing region leading to spontaneous ignition. To shut down the rig quickly should these problems arise, a potentiometric temperature controller was connected to the thermocouple just upstream of the flameholder. In the event of flashback or preignition (and consequent increase in the premixing region temperature) the temperature controller was designed to shut off the fuel solenoid valve.

#### 5.5 Experimental Procedures

##### 5.5.1 Fuel and Equivalence Ratio Determination

The use of a gaseous fuel avoids the problem of vaporizing a conventional liquid fuel and simulates a prevaporized system. Propane has a heating value near that of jet aircraft fuels so that combustion characteristics, especially  $\text{NO}$  production, are similar. Marek and Papathakos (9) showed that emission levels from burning Jet A fuel agree well with results from gaseous propane fuel.

It was important to determine if the emissions measured from the gas sample probe on the center line were representative of the average concentrations in the exhaust. For this purpose an equivalence ratio based on the measured exhaust gas species concentrations was compared with that from fuel and air flow rate measurements. The comparison is shown in Figure 21 for various inlet conditions. Agreement between the two equivalence ratios was generally within 5 percent showing that the single centerline probing was able to provide a good sample for analysis.

The experimental procedures for determining the lean ignition and blow-out limits of the fuel-air mixture for various inlet conditions (the test matrix is given in Table 2) are given below.

##### 5.5.2 Lean Ignition Limit

To determine the lean ignition limit, the premixing length, the air

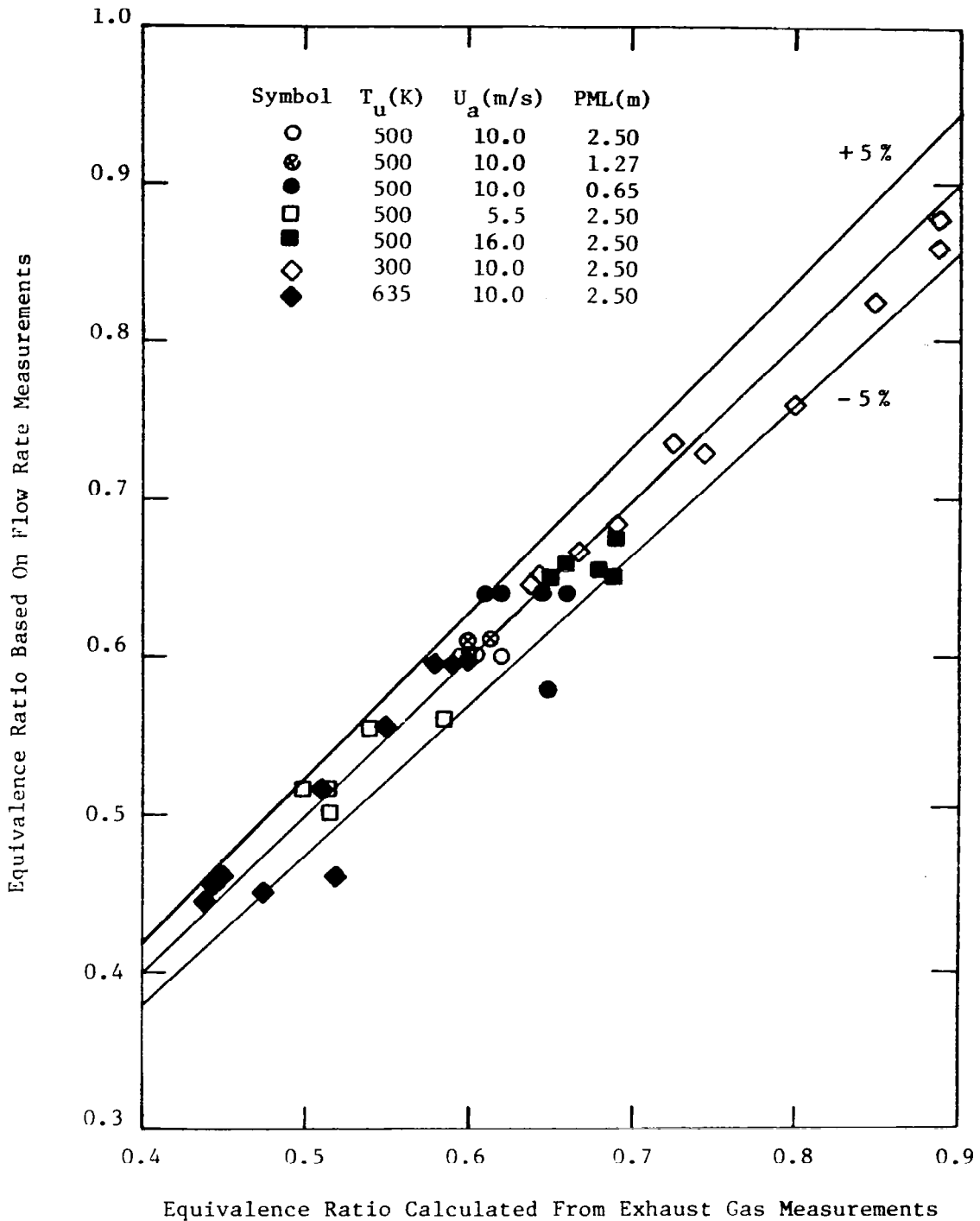


Figure 21

Comparison of Equivalence Ratios based on Fuel and Air Flow Rate Measurements with those Calculated from Exhaust Gas Measurements.

velocity and inlet temperature were set at the desired values\*. The igniters were switched on and the fuel flow rate was gradually increased until a flame was visible in the apparatus, its presence made apparent as a bluish hue around the spark. A further increase in the fuel flow rate resulted in propagation of the flame into the main stream. In most cases this development occurred over a small increase in the fuel flow rate. In all cases, successful ignition was taken to occur when the flame was self-sustaining with the igniters switched off. The ignition limit as defined above is, therefore, the minimum fuel flow rate required for a self-sustaining flame.

This operating procedure for observing ignition has been used by others in the field (93-95). It is recognized that this technique may yield somewhat subjective ignition limits. This procedure was, however, satisfactory in that the data scatter, both from run to run on the same day and from day to day, was smaller than the estimated accuracy of the (air and fuel flow rate) metering devices. In order to make the measurement as objective as possible, the apparatus was designed such that the operator could not see the fuel-metering device and the flame at the same time. Also, independent judgements by a secondary observer did not produce consistently different ignition limits.

### 5.5.3 Lean Blowout Limit

The usual practice in determining the lean blowout limit is to decrease the fuel flow rate (with the igniters switched off) until the flame blows off (e.g. (26)). However, in order to make the sequence for obtaining this limit less subjective, we adopted a procedure based on the observed behavior near blowout. Marek and Papathakos (9) report that the combustion efficiency of a premixed Jet-A fueled combustor remained at over 99 percent as the fuel-air mixture was made leaner until very close to the blowout limit, when it dropped rapidly. The blowout limit was, therefore, determined by continuously monitoring the concentration of unburned hydrocarbons (HC) as the fuel flow rate was gradually decreased. After each decrease, a delay of 1 to 2 minutes was allowed before a further decrease.

Figure 22 shows plots of HC concentration versus fuel-air equivalence ratio ( $\phi$ ). We notice that the HC levels show practically no change with  $\phi$  until at some value of  $\phi$  they increase rapidly. The equivalence ratio at which this steep increase occurs is defined as the lean blowoff limit. This large increase in HC values always coincided with the flame blowing off. The blowoff point was almost always abrupt and well defined. For some operating conditions the flame tended to lengthen and would move downstream, attach itself to the exhaust, and burn inside the exhaust chamber downstream of the burner.

The use of the opposite procedure for determining the lean blowout limit, namely, increasing the airflow rate for constant fuel flow rate, was explored,

---

\*

Since the fuel was not pre-heated, the inlet air temperature was always set a few degrees above the desired value. For all operating conditions, the mixture temperature and velocity were within  $\pm 7$  K and  $\pm 5\%$  respectively of the desired values.

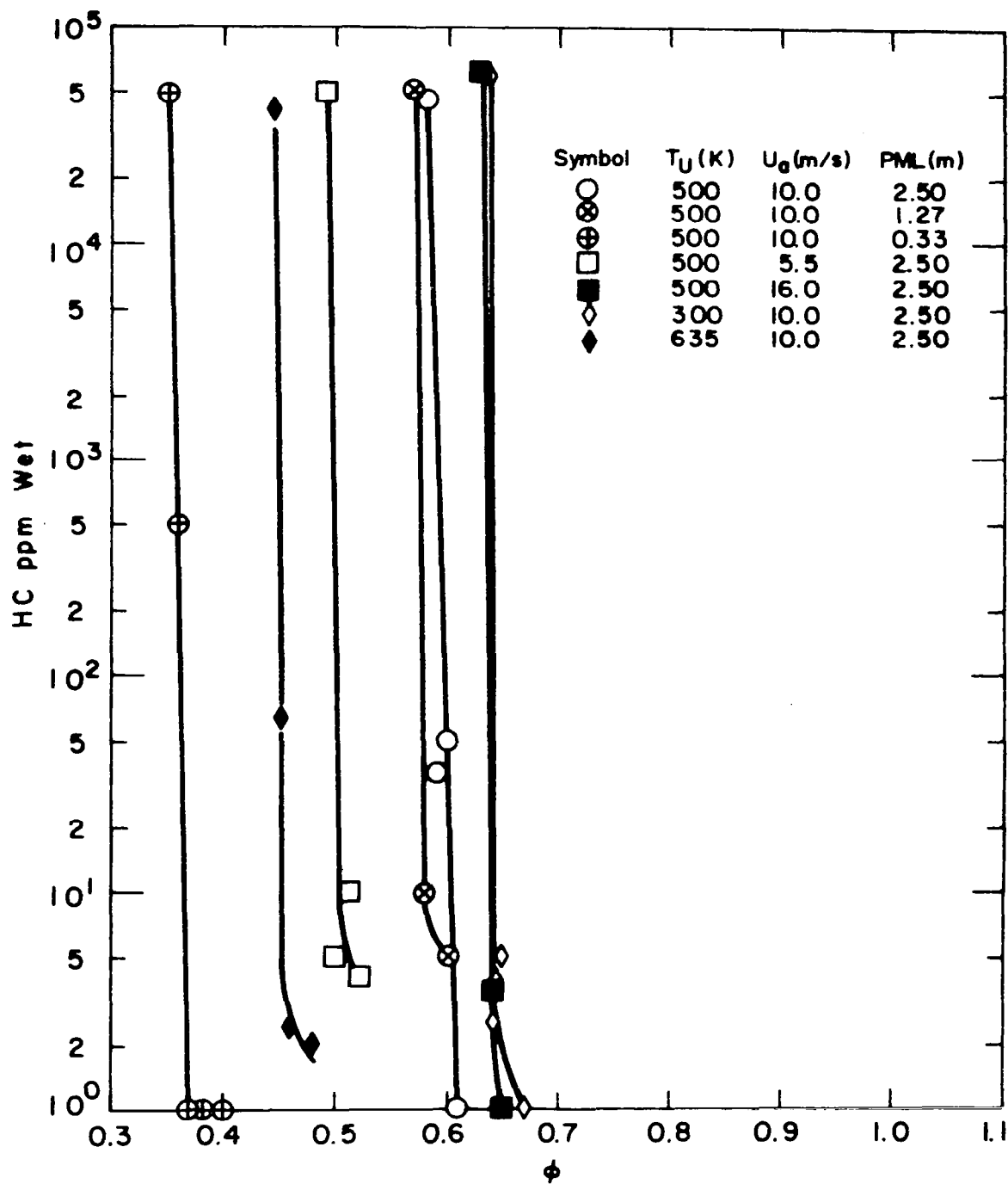


Figure 22 Plots of Unburned Hydrocarbon Concentration (HC) Against Equivalence Ratio, Near and at Blowout, for Different Inlet Conditions.

but had to be abandoned, since fine metering of the air flow rate was difficult. Although not well quantified (this procedure was attempted at only two operating points) this procedure gave the same results as decreasing the fuel flow rate. This agrees with the findings of DeZubay (26), Fetting et al (36) and Fillipi and Fabbrovich-Mazza (37) who showed that both procedures give equivalent blow-out results.

## 5.6 Operating Parameters

**Primary Variables:** The primary parameters that were varied in this study are: (i) air flow rate (velocity  $U_a$ ); (ii) mixture unburned temperature ( $T_u$ ); and (iii) premixing length (PML) - defined as the distance between the fuel injector and the flameholder. The pressure was fixed at one atmosphere.

**Secondary Variables:** In the course of the experimental work, several secondary variables were identified. Experimental work was carried out to determine the effect, if any, of these variables on the lean ignition and blowout limits. This was done to determine which variables could be discarded as having little or no effect on the limits and which had to be carefully controlled. These variables are identified and a summary of the observations is given below; details of the investigations are presented in reference 86.

The parameters studied were: combustor wall temperature, igniter electrode size, spark gap and location with respect to the flameholder, and flameholder water cooling. The results showed that the igniter electrode size, flameholder water cooling and location of the spark in relation to the flameholder have little or no effect on the ignition limit. However, for the ignition limits to represent the true ignition limit, the spark gap has to be greater than a critical value, and the temperature of the burner wall cannot be very high. Flameholder water cooling and the combustor wall temperature had little or no effect on the lean blowout limit. To prevent the igniter electrodes from significantly disturbing the flow field and from serving as secondary flameholders, thin wires were used. With thin electrodes, blowout limits generated with the igniter wires in the flame, and with the wires removed from the combustor, were identical. During facility development it was found that with increased noise intensity, the lean limits are significantly richer. A Helmholtz resonator was connected to the exhaust system for all the tests reported here to reduce acoustic effects to a minimum.

**Data Matrix:** A base operating condition ( $U_a = 10$  m/s,  $T_u = 500$ K and PML = 2.50 m) was established. The effects of each of the operating parameters on the lean ignition and blowout limits were studied by varying each operating parameter about the base operating condition. The data matrix is given in Table 2.

Table 2  
Data Matrix

Air Velocity $U_a$ (m/s)	Inlet Temperature $T_u$ (K)	Premixing Length PML (m)
5.5	500	2.50
*10.0	500	2.50
16.0	500	2.50
10.0	300	2.50
10.0	635	2.50
10.0	500	1.27
10.0	500	0.65
10.0	500	0.33

\* base operating condition

For all cases: P - 1 atm.

Fuel - commercial grade propane

## 6 RESULTS AND DISCUSSION

The lean ignition and blowout limits for a gaseous propane-air mixture were obtained for different inlet temperatures, reference velocities and pre-mixing lengths. For these inlet conditions, emission levels of unburned hydrocarbons (HC) carbon monoxide (CO) and nitrogen oxides ( $\text{NO}_x$ ) and concentrations of oxygen ( $\text{O}_2$ ) and carbon dioxide ( $\text{CO}_2$ ) were also measured. The variation of these species was measured by axially traversing the combustor with the exhaust gas sampling probe. All gas sampling was done along the burner centerline as it best approximates the results from an adiabatic burner (the total heat loss through the combustor walls and to the flameholder cooling water was estimated to be less than 5 percent.)

### 6.1 Measured Species Concentrations

In this section, we present the variation of the measured species concentrations with axial distance from the flameholder. The measurements of HC were made on a wet basis and those of  $\text{O}_2$ ,  $\text{NO}_x$ , CO and  $\text{CO}_2$  were made on a dry basis. From the raw data obtained from these measurements, the equivalence ratio ( $\phi_c$ ) was calculated using the procedure described by Bigio (96).

The data obtained from these measurements and calculations are presented as follows. Plotted in Figure 23 are the concentrations of HC,  $\text{O}_2$ ,  $\text{CO}_2$ , CO and  $\text{NO}_x$  and  $\phi_c$  against  $z/D$ , for the base operating condition (see Table 2);  $z$  is the axial location of the probe and  $D$  is the combustor diameter. We then present only those species for the other operating conditions that showed a significantly different behavior from this base data. The only operating parameter that had a significant effect on the shapes of the species concentration versus  $z/D$  curves was the premixing length, PML. The nature of these curves for the base operating condition, and the reasons for significant deviations from this behavior, are discussed below.

**Unburned Hydrocarbons (HC):** This plot shows the characteristic decay of HC concentration with distance from the flameholder as the propane fuel continues to react to form lower hydrocarbons which in turn are oxidized. The point shown  $z/D = 0$  is the calculated HC concentration for the mean equivalence ratio ( $\bar{\phi}_c$ ) assuming an unreacted fuel-air mixture. For most of the operating conditions, the HC concentration levels reach a few ppm (from between 70,000 and 80,000 ppm) within one burner diameter downstream of the flameholder. The measurements of HC concentrations of a few ppm were marked by a good deal of data scatter. This plot also illustrates the difficulty of probing in and close to the recirculation zone; it is unclear exactly where the gas sample originates.

**Carbon Monoxide (CO):** The plot of CO against  $z/D$  shows the characteristic decay of CO concentration with distance from the flameholder, as a result of oxidation of CO to  $\text{CO}_2$ . The effect - of decreasing PML - on the CO concentration is shown on Figure 24. Also shown for all operating conditions (except  $\text{PML} = 0.33$ ) are the equilibrium levels of CO for the average calculated equivalence ratio ( $\bar{\phi}_c$ ) and the appropriate inlet temperature ( $T_u$ ).

$T_U = 500 \text{ K}$ ,  $P = 1 \text{ atm.}$ ,  $U_{a-} = 10 \text{ m/s}$ ,  $PML = 2.50 \text{ m}$   
 $\phi_m = 0.60$ ,  $\phi_c = 0.607$

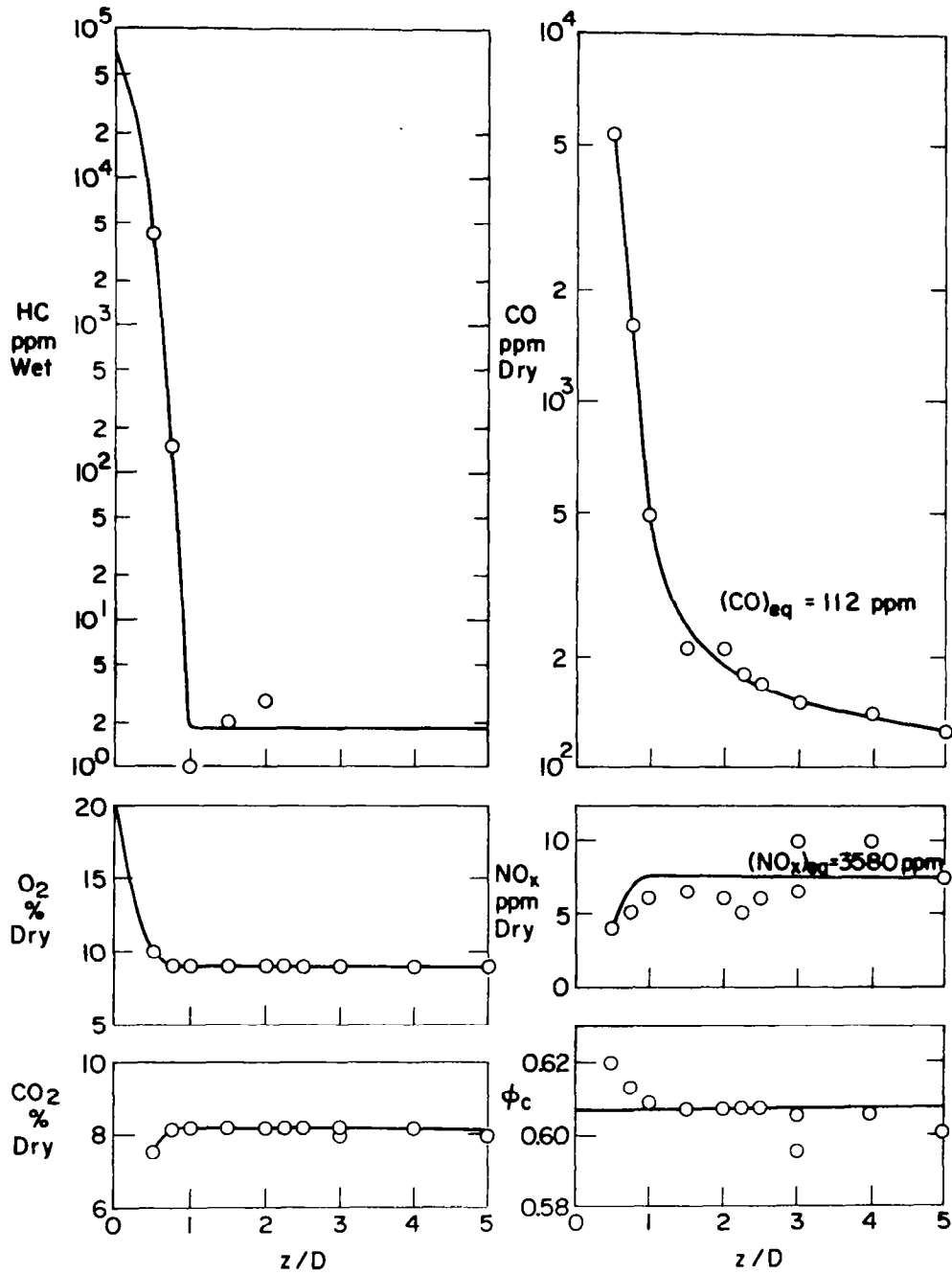


Figure 23 Plots of HC,  $O_2$ ,  $CO_2$ , CO and  $NO_x$  Concentrations and  $\phi_c$  Against  $z/D$  for the Base Operating Condition.



Decreasing the premixing length results in higher values of the CO emission levels. We notice that, for PML = 2.50 m, the CO values tend towards the equilibrium value of about 110 ppm. However, for premixing lengths less than this, the values remain above equilibrium. In order to account for the different values of  $\bar{\phi}_C$ , a plot of CO divided by the equilibrium value is shown in Figure 25. No plot is shown for the case PML = 0.33 m because no value for  $\bar{\phi}_C$  (and hence CO equilibrium value) could be assigned. As shown later, large-scale nonuniformities are present for this condition. We see from Figure 25 that for PML = 2.5 m, within experimental errors, the CO has reached the equilibrium level by  $z/D$  of about 4.

Bigio (96) has shown that, for lean mixtures, nonuniformities significantly increase the CO concentration levels. This fact, coupled with the discussion above on the variation of CO with PML, implies that increasing PML increases the fuel-air mixture uniformity.

Oxygen ( $O_2$ ) and Carbon Dioxide ( $CO_2$ ): These species are the major combustion products measured directly. The point on the  $O_2$  concentration versus  $z/D$  curve at  $z/D = 0$  is the calculated  $O_2$  concentration for the mean calculated equivalence ratio ( $\bar{\phi}_C$ ), assuming an unreacted fuel-air mixture (Figure 23). These plots show that the  $O_2$  and  $CO_2$  concentrations reach their steady state values within one diameter downstream of the flameholder.

Shown on Figure 24 are the effects - of decreasing PML - on the  $O_2$  concentration versus  $z/D$  curves. The points at  $z/D = 0$  are calculated  $O_2$  concentration for  $\bar{\phi}_C$  assuming an unreacted fuel-air mixture; for PML = 0.33 m, this was calculated for the measured equivalence ratio ( $\phi_m$ ). The curve  $O_2$  versus  $z/D$  for the premixing length of 0.33 m displays a radically different behavior. The  $O_2$  level decreases up to  $z/D$  of about 1 and then continues to increase with increasing distance from the flameholder. This behavior can be explained by referring to the plots of HC (Figure 23) and  $\phi_C$  against  $z/D$  (Figure 26). Notice that the HC has virtually disappeared by  $z/D$  of about 1. This explains the  $O_2$  decrease up to  $z/D$  of 1. The calculated equivalence ratio ( $\phi_C$ ) for this case is not uniform indicating the presence of large scale nonuniformities. As these large scale nonuniformities mix out,  $\phi_C$  decreases towards its average measured value. This decrease in the value of  $\phi_C$  is responsible for the increase in oxygen concentration.

Calculated Equivalence Ratio ( $\phi_C$ ): These plots (Figures 23 and 26) show that, within the data scatter, the equivalence ratio is uniform along the axis of the combustor for all cases except PML = 0.33 m. We concluded from the behavior of the CO levels with premixing length that increasing PML increases the mixture uniformity. This conclusion coupled with the uniformity of  $\phi_C$  with  $z/D$  implies that the nonuniformities introduced by shortening the premixing length are on the small turbulence scales. Shortening the premixing length to 0.33 m, however, introduces large-scale nonuniformities. For this premixing length, the centerline is richer than the average equivalence ratio (measured value: 0.64). Because of mixing downstream of the flameholder, these large scale nonuniformities mix out, leading to a decrease in the calculated equivalence ratio.

Nitrogen Oxides ( $NO_x$ ): The plot of  $NO_x$  concentration versus  $z/D$  shows the char-

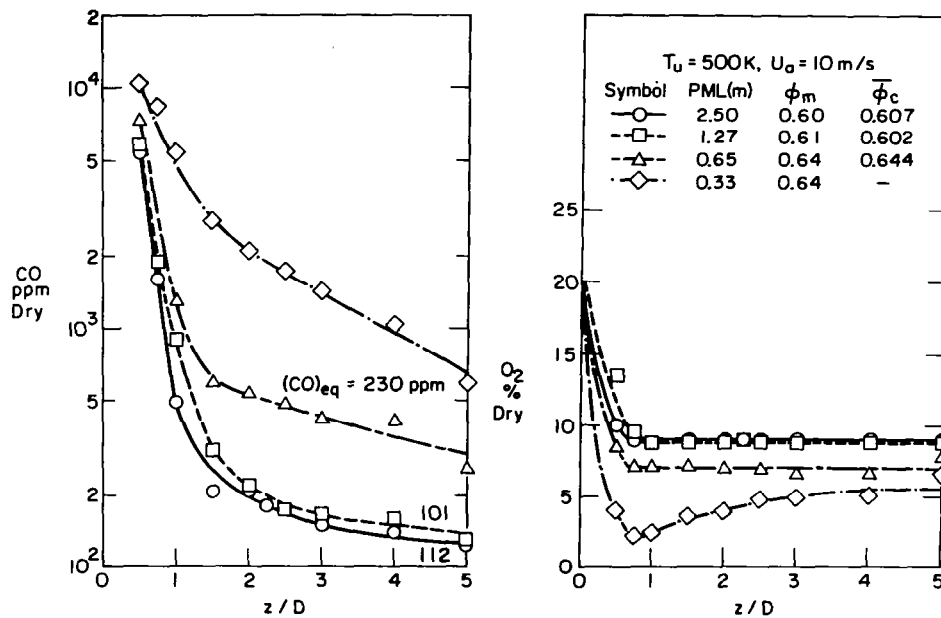


Figure 24 Variations of CO and O<sub>2</sub> Concentrations with  $z/D$  for Different Premixing Lengths.

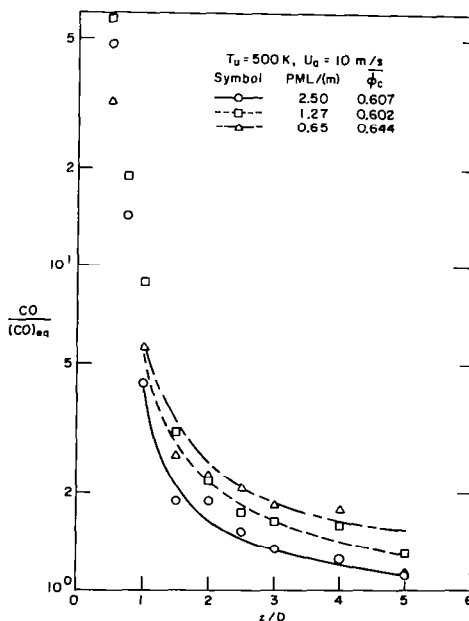


Figure 25 Plots of CO Concentration Divided by Equilibrium CO Concentration at  $\phi_c$  and  $T_u$ , for Different Premixing Lengths.

acteristic increase in  $\text{NO}_x$  concentration with distance from the flameholder. This increase in  $\text{NO}_x$  is a result of chemical reactions between free radicals and the oxygen and nitrogen in the combustion air. These reactions are relatively slow, explaining observed values very much lower than the equilibrium value indicated against the curve (Figure 23). The equilibrium value was calculated for  $\bar{\phi}_c$  and  $T_u$ . This plot also indicates, by the large data scatter, the experimental difficulty in measuring such low levels of  $\text{NO}_x$ .

Decreasing the premixing length (and hence increasing the mixture non-uniformity) has a significant effect on the  $\text{NO}_x$  levels (Figure 26). Shown against each curve is the equilibrium value of  $\text{NO}_x$  concentration calculated for appropriate values of  $\bar{\phi}_c$  and  $T_u$ : for PML = 0.33 m,  $\phi_m$  was used. For these values of PML, the calculated Emission Indices of the  $\text{NO}_x$  ( $\text{EI}_{\text{NO}}$ ) are given in Table 3. We notice that ( $\text{EI}_{\text{NO}}$ ) jumps from a value of 0.19 to 1.71 gNO/kg fuel. A direct comparison of these numbers is complicated by the fact that  $\bar{\phi}_c$  (or  $\phi_m$ ) is different for the shorter premixing lengths from the longer ones. However, Mikus et al (11) have demonstrated that, for lean mixtures, nonuniformities significantly increase  $\text{NO}_x$  emission levels.

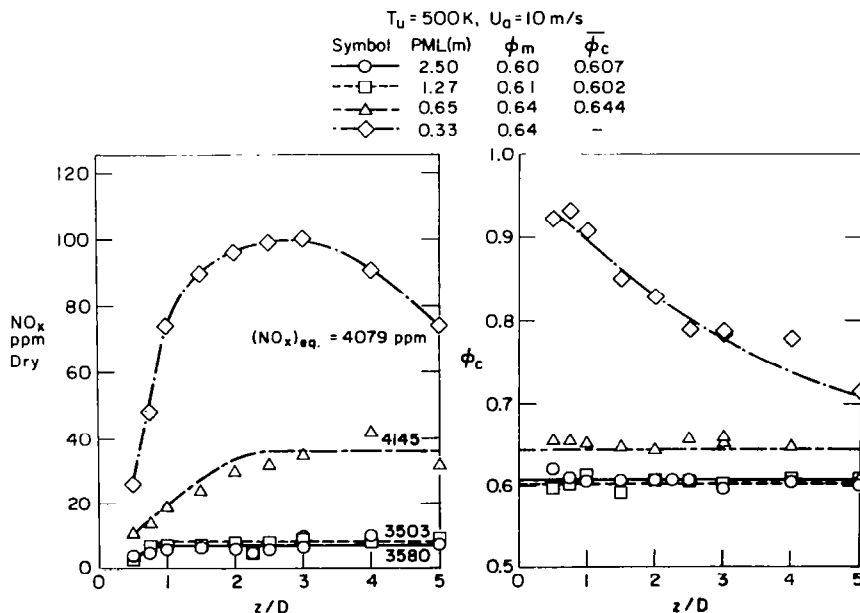


Figure 26 Variations of  $\text{NO}_x$  Concentration and  $\phi_c$  with  $z/D$  for Different Premixing Lengths.

Table 3  
Effect of Premixing Length on NO<sub>x</sub> Emission Levels

Premixing Length PML (m)	Average Calculated $\phi$ From Exhaust Gas Measurements, $\phi_c$	NO <sub>x</sub> Emission Level At Combustor Exit PPM Dry	EI <sub>NOX</sub> g <sub>NO</sub> /kg Fuel
2.50	0.607	7.5	0.19
1.27	0.602	8.5	0.22
0.65	0.644	36.0	1.03
0.33	0.640*	75.0	1.71

\* Measured equivalence ratio,  $\phi_m$

for all cases: (i)  $T_u = 500$  K,  $P = 1$  atm.,  $U_a = 10$  m/s

(ii) fuel: commercial grade propane

## 6.2 Lean Ignition and Blowout Limits: Parameteric Study and Comparison with Model Predictions

In this section, the experimental lean ignition and blowout limits obtained for the conditions listed in the data matrix are presented and, where possible, quantitative comparisons are made with the stochastic mixing model predictions. For each operating condition, the lean ignition and blowout limits were obtained following the procedures given in section 5.5. The effects on the lean limits of the parameters varied for this study are discussed below.

**Velocity:** Shown on Figure 27 are the model predictions and the experimental data for the variation of the lean limits with velocity for  $T_u = 500$  K, PML = 2.5 m. Increases in mixture velocity lead to faster mixing rates and smaller residence times; hence the requirement for richer mixtures. We notice that the model predictions of the blowoff limits compare very favorably with the experimental values; however, the predicted lean ignition limits are richer than the experimental values. This is consistent with the findings of Wear and Jones (97) who showed that the ignition data for propane were markedly superior to (i.e. lower than) that of natural gas fuel. They attribute this difficulty in igniting methane to its stability. Karpov and Sokolik (98) have also experimentally demonstrated that the lean ignition limits for methane/air mixtures are richer than those for propane/air mixtures. Although the predicted ignition limits are richer than the experimental limits, the slopes of the two lines with respect to the velocity are about the same.

**Inlet Temperature:** The effect of varying the inlet temperature ( $T_u$ ) was studied for a velocity of 10 m/s and a premixing length of 2.5 m. With increased  $T_u$ , both ignition and blowout limits are leaner (see Figure 28) because of increased burning rates. The agreement between the model predictions and the blowout data is again satisfactory; for reasons given above, the predicted ignition limits are richer.

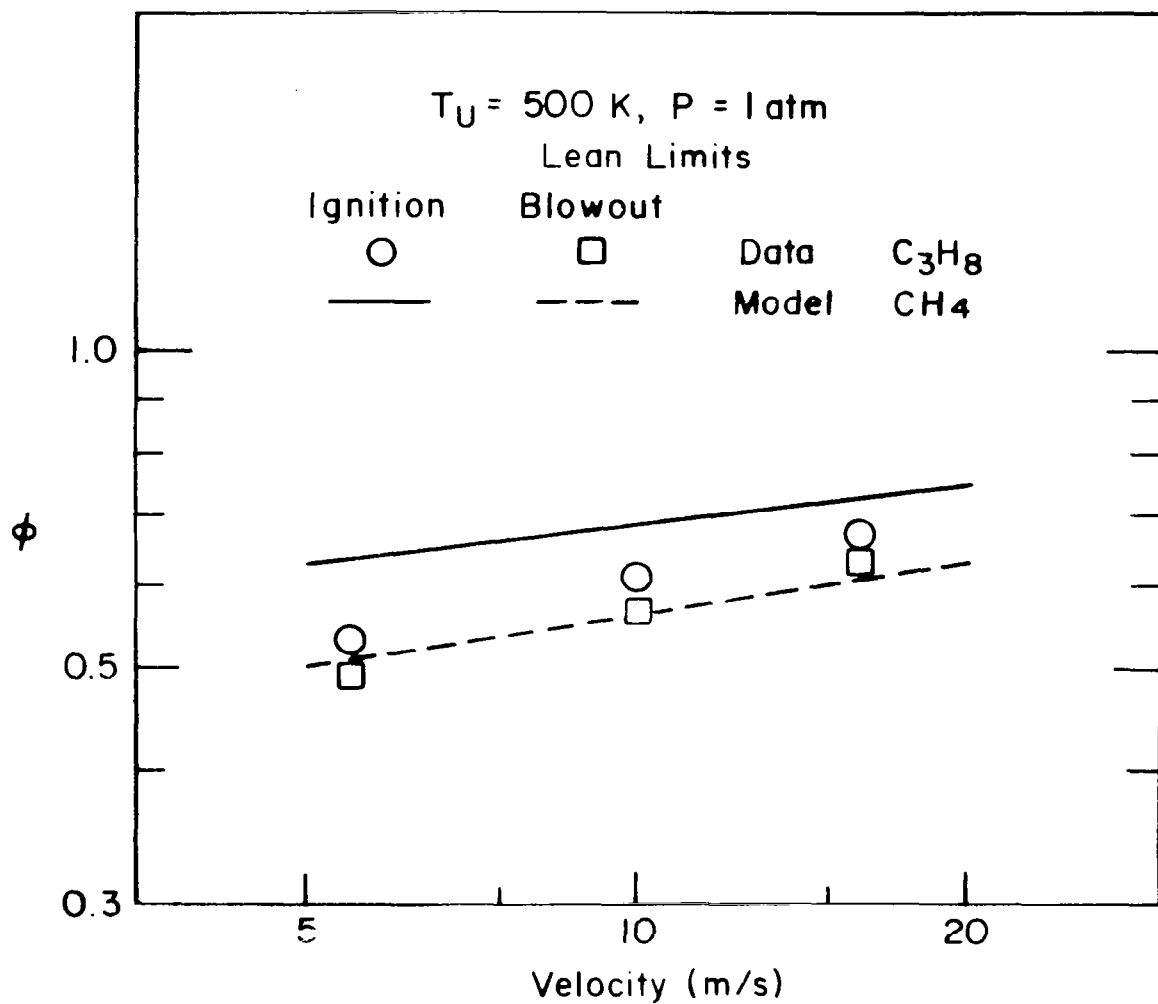


Figure 27

Variations of Measured and Predicted Lean Ignition and Blowout Limits of Uniform Mixtures with Inlet Velocity.

Premixing length: The effect of changing the premixing length is shown in Figure 29. Notice that decreasing PML has a very strong effect on the limits; they are significantly reduced. The lines connecting the experimental values are not extended to include the values for PML = 0.33 m. The reason for this is as follows. The aim of this thesis was to study the effect of small-scale turbulent concentration nonuniformities on the lean ignition and blowout limits. However, as shown in section 6.1, for PML = 0.33 m, large-scale concentration nonuniformities were present in the burner. The data points for this premixing length are not, therefore, completely consistent with the rest of the data where no large-scale nonuniformities were present.

We showed in section 6.1 that decreasing premixing length increases the (small-scale) concentration nonuniformity of the mixture. We can therefore conclude that concentration nonuniformities significantly reduce the lean ignition and blowout limits. Decreasing PML from 2.5 m to 0.65 m results in about a 15 percent decrease in the fuel flow rate required for a stable flame.

Bigio (96) quantified small-scale nonuniformities by assuming the Gaussian distribution given by Equation 14 for fuel fraction. He then calculated the value of the unmixedness parameter  $s$  by matching the measured time-average  $\text{CO}_2$ ,  $\text{CO}$  and  $\text{O}_2$  concentrations with those calculated from the Gaussian distribution together with the equilibrium concentrations of these species as a function of equivalence ratio. He found that, for lean mixtures, the  $\text{O}_2$  and  $\text{CO}_2$  values were insensitive to values of  $s$ . The only specie that can therefore be used for such a calculation, with the data reported here, is  $\text{CO}$ . But, as we saw in section 6.1, for  $T_u = 500$  K,  $U_a = 10$  m/s, PML = 2.5 m, the  $\text{CO}$  level reached near equilibrium values only at  $z/D = 4$ . The calculation of  $s$ , was therefore carried out with the data at  $z/D = 4$ . The  $s$  values from these calculations were found to be 0.06 and 0.10 respectively for PML = 1.27 and 0.65 m. Because of mixing downstream of the flameholder, the mixture is expected to become better mixed as it moves downstream. We can conclude therefore that for PML values of 0.65 and 1.27 m, values of  $s$  in the recirculation zone are greater than 0.1 and 0.06 respectively.

From Figure 15, which shows the dependence of the lean ignition limit on  $s$ , we see that for a 15 percent reduction in the lean ignition limit,  $s$  has to have a value of about 0.2 in the incoming unburnt fuel-air mixture. Compare this figure to 0.1 at an axial location 4 burner diameters downstream of the flameholder. Because of mixing within and downstream of the recirculation zone,  $s$  may well decrease to a value of 0.1 at an axial location 4 diameters downstream of the flameholder.

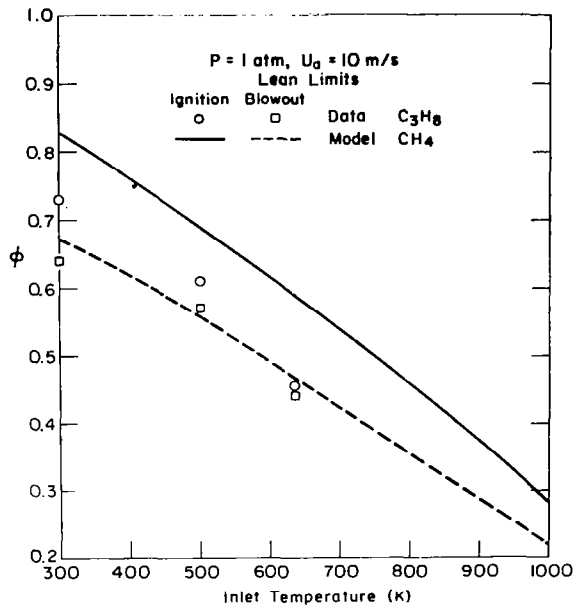


Figure 28 Variations of Measured and Predicted Lean Ignition and Blowout Limits of Uniform Mixtures with Inlet Temperature.

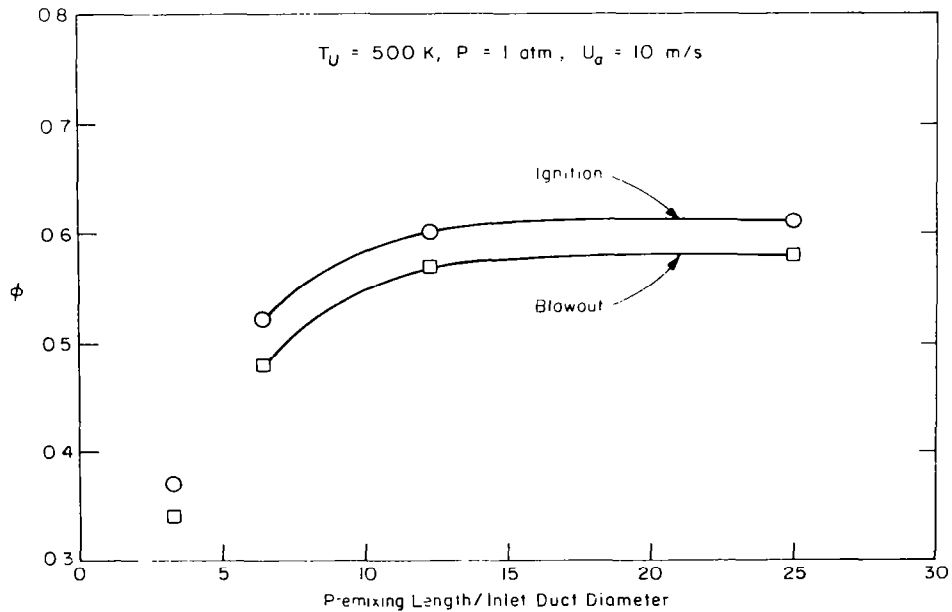


Figure 29 Variations of Measured Lean Ignition and Blowout Limits with Premixing Length.

## 7 CONCLUSIONS

Models for predicting ignition and blowout limits in a combustor recirculation zone have been developed. One of these, a correlation for the blowoff velocity of premixed turbulent flames stabilized by bluff bodies, has been derived using the basic quantities of turbulent flow, and the laminar flame speed.

The predicted variations of the blowoff velocity with equivalence ratio, mixture temperature and pressure, flameholder characteristic dimension, and turbulent Reynolds number were compared with experimental data in the literature and good agreement was obtained. Using the velocity in the plane of the flame holder and the recirculation zone length as the characteristic flow velocity and the length scale, data on the blowoff velocity divided by the flame speed for different flameholder and combustor geometries could be correlated over two orders of magnitude in Reynolds number.

A second model, a statistical model employing a Monte Carlo calculation procedure to follow the mixing process, was developed to account for fuel-air ratio nonuniformities in the combustor primary zone. An overall kinetic rate expression was used to describe the fuel oxidation process. The model was used to predict the lean ignition and blowout limits of premixed turbulent flames. The predicted trends with reference velocity, mixture pressure and temperature were in good agreement with experimental observations. The model was also used to study the effects of mixture nonuniformity on the lean ignition limit, using a Gaussian distribution to describe the fuel fraction distribution in the recirculation zone. The model predictions showed a significant reduction in the lean ignition limit with increased mixture nonuniformity.

In order to verify the trends predicted by the statistical mixing model, experimental work was carried out on a constant cross-sectional area tubular combustor. The primary variables varied were the reference velocity, mixture temperature and the length over which the fuel and air were allowed to mix. The aim of varying the premixing length was to study the effects of small-scale concentration nonuniformities on the lean ignition and blowout limits. The statistical mixing model predictions were compared with these experimental results. The predicted trends with velocity and temperature of the lean ignition and blowout limits of uniform mixtures were shown to be in good agreement with the experimental observations. The agreement between the predicted and measured blowout limits was good; however, the model predicted higher lean ignition limits than were obtained experimentally. This difference was attributed to the different fuels used in the modelling studies and the experimental work. Although quantitative comparisons between the model predictions and experimental findings on the effect of mixture nonuniformity on the lean ignition limit could not be made, the trends were similar; both show a significant reduction in the lean ignition limit with increased mixture nonuniformity.

The following specific conclusions can be drawn from this study:



(a) **Blowoff Velocity Correlation:**

- (i) Although the mechanism of flame stabilization in a recirculation zone is a complex process involving both aerodynamic and chemical reaction processes, at blowout with premixed fuel-air mixtures, these effects can be separated into characteristic mixing and chemical times.
- (ii) The velocity in the plane of maximum flameholder blockage is a better measure of the blowoff velocity than the approach flow velocity.
- (iii) The length of the recirculation zone downstream of a flameholder is a more appropriate length scale for defining the flameholder stability characteristics than its geometric size, although the latter is a more easily measurable quantity.

(b) **Statistical Model Calculations:**

- (i) This model can be used as an interpolative and extrapolative tool for studying the lean ignition and blowout limits of uniform mixtures.
- (ii) The model provides a means of accounting for fuel-air ratio non-uniformities in the unburned mixture.
- (iii) Increasing mixture nonuniformity leads to a significant reduction in the lean ignition limit.

(c) **Experimental Work:**

- (i) Increasing the distance over which the fuel and air mix (i.e. for constant velocity, increasing the residence time in the mixing zone) leads to a more uniform mixture.
- (ii) Increasing mixture nonuniformity leads to a substantial reduction in the lean ignition and blowout limits.
- (iii) Mixture nonuniformities cause a substantial increase in the emission levels of nitrogen oxides for lean mixtures. Low  $\text{NO}_x$  emissions, therefore, require the combustion zone to be lean and well mixed.

## REFERENCES

1. Grobecker, A.J., Coroniti, S.C. and Cannon, R.H.Jr., "Report of Findings - The Effects of Stratospheric Pollution by Aircraft", Executive Summary, U.S. Department of Transportation, DOT-TST-75-50, December 1974.
2. "Lean Premixed/Prevaporized Combustion," A workshop held at the National Aeronautics and Space Administration, Lewis Research Center, Cleveland, Ohio, January 20-21, 1977, NASA CP-2016.
3. Ferri, A., "Better Marks on Pollution for the S.S.T.," Aeronautics and Astronautics, July 1972.
4. Ferri, A. and Roffe, G., "Low NO<sub>x</sub> Combustion Processes," 75th National Meeting, A.I.Ch.E., June 1973.
5. Anderson, D.N., "Effect of Premixing on Nitric Oxide Formation," NASA Technical Memorandum, TM-X-68220, 1973.
6. Anderson, D.N., "Effects of Equivalence Ratio and Dwell Time on Exhaust Emissions from an Experimental Premixing Prevaporizing Burner," NASA Technical Memorandum, TM-X-71592, 1975.
7. Roffe, G. and Ferri, A., "Prevaporizing and Premixing to Obtain Low Oxides of Nitrogen in Gas Turbine Combustors," NASA Contractor Report CF-2495, March 1975.
8. Roffe, G. and Ferri, A., "Effect of Premixing Quality on Oxides of Nitrogen in Gas Turbine Combustors," NASA Contractor Report CR-2657, February 1976.
9. Marek, C.J. and Papathakos, L.C., "Exhaust Emissions from a Premixing Prevaporizing Flame Tube Using Liquid Jet A Fuel," NASA Technical Memorandum TM X-3383, February 1976.
10. Beer, J.M. and Chigier, N.A., Combustion Aerodynamics, Interscience Publishers Limited, 1972.
11. Mikus, T., Heywood, J.B. and Hicks, R.E., "Nitric Oxide Formation in Gas Turbine Engines: A Theoretical and Experimental Study," NASA Contractor Report CR-2977, April 1978.
12. Odgers, J., "Current Theories of Combustion within Gas Turbine Combustors," Fifteenth Symposium (International) on Combustion, 1974, pp.1321-1338.
13. Flagan, R.C. and Appleton, J.P., "A Stochastic Model of Turbulent Mixing with Chemical Reaction: Nitric Oxide Formation in a Plug-Flow Burner," Combustion and Flame, Vol. 23, 1974, pp. 249-267.

14. Longwell, J.P., "Flame Stabilization by Bluff Bodies and Turbulent Flames in Ducts," Fourth Symposium (International) on Combustion, The Williams and Wilkins Company, Baltimore, Maryland, 1953, pp. 90-97.
15. Longwell, J.P., "Combustion Problems in the Ramjet," Fifth Symposium (International) on Combustion, Reinhold Publishing Corporation, New York, 1955, pp.48-56.
16. Penner, S.S. and Williams, F., "Recent Studies on Flame Stabilization of Premixed Turbulent Gases," Applied Mechanics Reviews, Volume 10, No. 6, June 1957, pp. 229-237.
17. Williams, F.A., "Flame Stabilization of Premixed Turbulent Gases," Applied Mechanics Surveys, Spartan Books, Washington, D.C., 1966, pp. 1157-1170.
18. Ozawa, R.I., "Survey of Basic Data on Flame Stabilization and Propagation for High Speed Combustion Systems," The Marquardt Company Technical Report AFAPL-TR-70-81, January 1971.
19. Wolfhard, H.G., Z. Technische Physik, 24, 1943, pp. 206-211.
20. Childs, J.H., McCafferty, R.J. and Surine, O.W., "Effect of Combustor-Inlet Conditions on Performance of an Annular Turbojet Combustor," NACA TN No. 1357, 1947.
21. Haddock, G.W. and Childs, J.H., "Preliminary Investigation of Combustion in Flowing Gas with Various Turbulence Promoters," NACA Research Memorandum, NACA RM Mo. E8C02, June 1948.
22. Scurlock, A.C., "Flame Stabilization and Propagation in High Velocity Gas Streams," Meteor Report No. 19, Fuels Lab, Massachusetts Institute of Technology, Cambridge, Massachusetts, May 1948.
23. Williams, G.C., Hottel, H.C. and Scurlock, A.C., "Flame Stabilization and Propagation in High Velocity Gas Streams," Third Symposium (International) on Combustion, The Williams and Wilkins Company, Baltimore, Maryland, 1949, pp. 21-40.
24. Longwell, J.P., Chenevey, J.E., Clark, W.W. and Frost, E.E., "Flame Stabilization by Baffles in a High Velocity Gas Stream," Third Symposium (International) on Combustion, The Williams and Wilkins Company, Baltimore, Maryland, 1949, pp. 40-44.
25. Nicholson, H.M. and Field, J.P. "Some Experimental Techniques for the Investigation of the Mechanism of Flame Stabilization in the Wakes of Bluff Bodies," Third Symposium (International) on Combustion, The Williams and Wilkins Company, Baltimore, Maryland, 1949, pp. 44-68.

26. DeZubay, E.A., "Characteristics of Disk-Controlled Flame," *Aero Digest*, 61, No. 1, 1950, p. 54.
27. Haddock, G.W., "Flame-Blowoff Studies of Cylindrical Flameholders in Channeled Flows," Progress Report No. 3-24, Jet Propulsion Laboratory, California Institute of Technology, Pasadena, California, May 1951.
28. Williams, G.C. and Shipman, C.W., "Some Properties of Rod-Stabilized Flames of Homogeneous Gas Mixtures," Fourth Symposium (International) on Combustion, The Williams and Wilkins Company, Baltimore, Maryland, 1953, pp. 733-742.
29. Russi, M.J., Cornet, I. and Cornog, R., "The Influence of Flame Holder Temperature on Flame Stabilization," Fourth Symposium (International) on Combustion, The Williams and Wilkins Company, Baltimore, Maryland, 1953, pp. 743-748.
30. Barrere, M. and Mestre, A., "Stabilization des Flammees par des Obstacles," Selected Combustion Problems -- Fundamentals and Aeronautical Applications, Butterworth's Scientific Publications, London, England, 1954, pp. 421-446.
31. Mestre, A., "Etude des Limites de Stabilite avec la Resistance des Obstacles a l'Ecoulement," Combustion Researches and Reviews, Butterworth's Scientific Publications, London, England, 1955, pp. 72-86.
32. Zukoski, E.E. and Marble, F.E., "The Role of Wake Transition in the Process of Flame Stabilization of Bluff Bodies," Combustion Researches and Reviews, Butterworth's Scientific Publications, London, England, 1955, pp. 167-180.
33. Zukoski, E.E. and Marble, F.E., "Experiments concerning the Mechanism of Flame Blowoff from Bluff Bodies," Proceedings of the Gas Dynamics Symposium on Aerothermochemistry, Northwestern University, Evanston, Illinois, 1956, pp. 205-210.
34. Westenberg, A.A., Berl, W.G. and Rice, J.L., "Studies of Flow and Mixing in the Recirculation Zone of Baffle-Type Flameholders," Proceedings of the Gas Dynamics Symposium on Aerothermochemistry, Northwestern University, Evanston, Illinois, 1956, pp. 211-219.
35. Petreiu, R.J., Longwell, J.P. and Weiss, M.A., "Flame Spreading from Baffles," *Jet Propulsion*, Vol. 26, 1956, pp. 81-97.
36. Fetting, F., Choudhury, A.P.R. and Wilhelm, R.H., "Turbulent Flame Blowoff Stability Effect of Auxilliary Gas Addition into Separation Zone," Seventh Symposium (International) on Combustion, Butterworth's Scientific Publications, London, England, 1959, pp. 621-632.

37. Fillipi, F. and Fabbrovich-Mazza, L., "Control of Bluff Body Flameholder Stability Limits," Eight Symposium (International) on Combustion, The Williams and Wilkins Company, Baltimore, Maryland, 1962, pp.956-963.
38. Winterfeld, G., "On Processes of Turbulent Exchange Behind Flameholders," Tenth Symposium (International) on Combustion, The Combustion Institute, 1965, pp. 1265-1275.
39. Kundu, K.M., Bannerjee, D., and Bhaduri, D., "Theoretical Analysis on Flame Stabilization by a Bluff Body," Combustion Science and Technology, 17, 1977, pp. 153-162.
40. Bovina, T.A., "Flame Stabilization in Boundary Layers," Combustion and Propulsion Third AGARD Colloquim, Noise-Shock Tubes-Magnetic Effects-Instability and Mixing, Pergamon Press, London, England, 1958, pp. 581-585.
41. Bovina, T.A., "Studies of Exchange Between Recirculation Zone Behind the Flame-holder and Outer Flow," Seventh Symposium (International) on Combustion, Butterworth's Scientific Publications, London, England, 1959, pp. 692-696.
42. Roffe, G. and Venkataramani, K.S., "Emission Measurements for a Lean Premixed Propane-Air System at Pressures up to 30 Atmospheres," General Applied Science Laboratories Inc. Technical Report, GASL TR-250, June 1978. (NASA Contractor Report CR-159421.)
43. Roffe, G. and Venkataramani, K.S., "Experimental Study of the Effect of Cycle Pressure on Lean Combustion Emissions," NASA Contractor Report 3032, July 1978.
44. Friedman, J., Bennet, W.J. and Zwick, E.B., "The Engineering Application of Combustion Research to Ramjet Engines," Fourth Symposium (International) on Combustion, The Williams and Wilkins Company, Baltimore, Maryland, 1953, pp. 756-764.
45. National Bureau of Standards: 65th Report of Progress on Combustion Chamber Research Program, March 1950.
46. Brown, G. and Roshko, A., "The Effect of Density Difference on Turbulent Mixing," AGARD Paper, CP-93, 23, 1971.
47. Brown, G. and Roshko, A., "On Density Effects and Large Structures in Turbulent Mixing Layers," J. Fluid Mechanics, 64, 1974, pp. 775-816.
48. Roshko, A., "Structure of Turbulent Shear Flows: A New Look," AIAA Journal, 14, October 1976, pp. 1349-1357.
49. Davies, P.O.A.L. and Yule, A.J., "Coherent Structures in Turbulence," J. Fluid Mechanics, 69, 1975, pp. 513-537.

50. Mollo-Christensen, E., "Intermittency in Large-Scale Turbulent Flows," Annual Review of Fluid Mechanics, 5, Annual Reviews, Palo Alto, 1973, pp. 101-118.
51. Winant, C.D. and Browand, F.K., "Vortex Pairing: The Mechanism of Turbulent Mixing-Layer Growth at Moderate Reynolds Number," J. Fluid Mechanics, 63, 1974, pp. 237-255.
52. Laufer, J., "New Trends in Experimental Turbulence Research," Annual Review of Fluid Mechanics, 7, Annual Reviews, Palo Alto, 1975, pp. 307-326.
53. Chomiak, J., "Dissipation Fluctuations and the Structure and Propagation of Turbulent Flames in Premixed Gases at High Reynolds Numbers, (International) Symposium on Combustion, The Combustion Institute, 1977, pp. 1665-1672.
54. Tabaczynski, R.J., Ferguson, C.R. and Radhakrishnan, K., "A Turbulent Entrainment Model for Spark-Ignition Engine Combustion," SAE Paper 770647, 1977.
55. Spalding, D.B., "Computer Modelling Techniques for Laminar and Turbulent Combustion," Central States Meeting, The Combustion Institute, Cleveland, Ohio, 1977.
56. Hires, S.D., Tabaczynski, R.J. and Novak, J.M., "Prediction of Ignition Delay and Combustion Intervals for a Homogeneous Charge, Spark Ignition Engine, SAE Paper 780232, 1978.
57. Townsend, A.A., Proceedings of the Royal Society, A208, 1951, p. 534.
58. Corrsin, S., "Turbulent Dissipation Fluctuations," Physics of Fluids, 5, 1962, pp. 1301-1302.
59. Tennekes, H., "Simple Model for the Small-Structure of Turbulence," Physics of Fluids, 11, 1968, pp. 669-671.
60. Kuo, A.Y.S. and Corrsin, S., "Experiments on Internal Intermittency and Fine-Structure Distribution Functions in Fully Turbulent Fluid," J. Fluid Mechanics, 50, 1971, pp. 285-319.
61. Kuo, A.Y.S. and Corrsin, S., "Experiments on the Geometry of the Fine-Structure Regions in Fully Turbulent Fluid," J. Fluid Mechanics, 56, 1972, pp. 447-479.
62. Tennekes, H. and Lumley, J.L., A First Course in Turbulence, Massachusetts Institute of Technology Press, Cambridge, Massachusetts, 1972.
63. Putnam, A.A. and Jensen, R.A., "Application of Dimensionless Numbers to Flashback and other Combustion Phenomena," Third Symposium (International) on Combustion, The Williams and Wilkins Company, Baltimore, Maryland, 1949, pp. 40-44.

64. Spalding, D.B., "Theoretical Aspects of Flame Stabilization, An Approximate Graphical Method for the Flame Speed of Mixed Gases," Aircraft Engineering, 25, 1953, p. 264.
65. Spalding, D.B., Some Fundamentals of Combustion, Academic Press Inc., New York, 1955.
66. Loblich, K.R., "Semi-Theoretical Consideration on Scaling Laws in Flame Stabilization," Ninth Symposium (International) on Combustion, Academic Press Inc., New York, 1963, pp. 949-957.
67. Andrews, G.E. and Bradley, D., "Determination of Burning Velocities: A Critical Review," Combustion and Flame, 18, 1972, pp. 133-153.
68. Andrews, G.E. and Bradley, D., "The Burning Velocity of Methane-Air Mixtures," Combustion and Flame, 19, 1972, pp. 275-288.
69. Lavoie, G.A., "Correlations of Combustion Data for S.I. Engine Calculations - Laminar Flame Speed, Quench Distance and Global Reaction Rates," SAE Paper 780229, 1978.
70. Ferguson, C.R. and Keck, J.C., "On Laminar Flame Quenching and its Application to Spark Ignition Engines," Combustion and Flame, 28, 1977, pp. 197-205.
71. Van Tiggelen, A. and Deckers, J., "Chain Branching and Flame Propagation," Sixth Symposium (International) on Combustion, Reinhold, New York, 1957, pp. 61-66.
72. Metghalchi, M. and Keck, J.C., "Laminar Burning Velocity of Isooctane-Air, Methane-Air and Methanol-Air Mixtures at High Temperature and Pressure," Chemical and Physical Processes in Combustion, The Eastern Section of the Combustion Institute, Hartford, Connecticut, November 10-11, 1977.
73. Glassman, I., Combustion, Academic Press Inc., New York, 1977, p. 68.
74. Tabaczynski, R.J., "Turbulence and Turbulent Combustion in Spark-Ignition Engines," Progress in Energy and Combustion Science, 2, 1976, pp. 143-165.
75. Longwell, J.P., "Flame Stabilization and Flame Propagation in Ramjet Combustors, Combustion Researches and Reviews," Butterworth's Scientific Publications, London, England, 1955, pp. 58-71.
76. Corrsin, S., "Statistical Behavior of a Reacting Mixture in Isotropic Turbulence," Physics of Fluids, Vol. 1, 1958, pp. 42-47.
77. Pratt, D.T., "Theories of Mixing in Continuous Combustion," Fifteenth Symposium (International) on Combustion, The Combustion Institute, 1975, pp. 1339-1351.

78. Pratt, D.T., "Mixing and Chemical Reaction in Continuous Combustion," Prog. Energy Combust, Sci., 1976, Vol. 1, pp. 73-86.
79. Komiyama, K., "The Effects of Fuel Injector Characteristics on Fuel-Air Mixing in a Burner," Ph.D. Thesis, Massachusetts Institute of Technology, Cambridge, Massachusetts, January 1975.
80. Schefer, R.W. and Sawyer, R.F., "Pollutant Formation in Fuel Lean Recirculating Flows," NASA Contractor Report, NASA CR-2785, December 1976.
81. Dryer, F.L. and Glassman, I., "The High Temperature Oxidation of CO and CH<sub>4</sub>," Fourteenth Symposium (International) on Combustion, The Combustion Institute, 1973, pp. 987-1003.
82. Glassman, I., Dryer, F.L. and Cohen, R., "Combustion of Hydrocarbons in an Adiabatic Flow Reactor: Some considerations and Overall Correlations of Reaction Rate," Presented at the Joint Meeting of the Central and Western States Sections of the Combustion Institute, San Antonio, Texas, April 21-22, 1975.
83. Hires, S.D., Ekchian, A., Heywood, J.B., Tabaczynski, R.J. and Wall, J.C., "Performance and NO<sub>x</sub> Emissions Modelling of a Jet Ignition Prechamber Stratified Charge Engine," SAE Paper 760161, 1976.
84. LoRusso, J., "Combustion and Emissions Characteristics of Methanol, Gasoline-Methanol, and Methanol Water Blends in a Spark Ignition Engine," S.M. Thesis, Dept. of Mechanical Engineering, Massachusetts Institute of Technology, Cambridge, Massachusetts, 1976.
85. Martin, M.K. and Heywood, J.B., "Approximate Relationships for the Thermodynamic Properties of Hydrocarbon-Air Combustion Products," Combustion Science and Technology, 15, 1977, pp. 1-10.
86. Radhakrishnan, K., "Premixing Quality and Flame Stability: A Theoretical and Experimental Study," Ph.D. Thesis, Dept. of Mechanical Engineering, Massachusetts Institute of Technology, Cambridge, Massachusetts, November 1978.
87. Anderson, D.N., "Effect of Hydrogen Injection on Stability and Emissions of an Experimental Premixed Prevaporized Propane Burner," NASA Technical Memorandum TMX-3301, October 1975.
88. Roffe, G. and Venkatramani, K.S., "Experimental Study of the Effects of Flameholder Geometry on Emissions and Performance of Lean Premixed Combustors," NASA Contractor Report CR-135424, June 1978.
89. Jones, G.W., Kennedy, R.E. and Spolan, I., "Effect of High Pressures on the Flammability of Natural Gas-Air-Nitrogen Mixtures," Bureau of Mines Report of Investigations 4557, November 1949.



90. Bolt, J.A. and Harrington, D.L., "The Effects of Mixture Motion Upon the Lean Ignition Limit and Combustion of Spark Ignited Mixtures," SAE Paper 670467, 1967.
91. Ballal, D.R. and Lefebvre, A.H., "The Influence of Flow Parameters on Minimum Ignition Energy and Quenching Distance," Fifteenth Symposium (International) on Combustion, The Combustion Institute, 1975, pp. 1473-1481.
92. Halstead, C.J. and Munro, A.J.E., "The Sampling, Analysis and Study of the Nitrogen Oxides Formed in Natural Gas/Air Flames," Proceedings, Conference on Natural Gas Research and Technology, Chicago, Illinois, February 28 - March 3, 1971.
93. Swett, C.C.Jr., "Spark Ignition of Flowing Gases Using Long-Duration Discharges," Sixth Symposium (International) on Combustion, Reinhold Publishing Corporation, New York, 1957, pp. 523-532.
94. Jensen, W.P. and Shipman, C.W., "Stabilization of Flame in High Speed Flow by Pilot Flames," Seventh Symposium (International) on Combustion, Butterworth's Scientific Publications, London, England, 1959, pp. 674-680.
95. Subba Rao, H.N. and Lefebvre, A.H., "Ignition of Kerosene Fuel Sprays in a Flowing Air Stream," Combustion Science and Technology, 8, 1973, pp. 95 - 100.
96. Bigio, D.I., "Fuel/Air Mixing Characteristics of Commercial Fuel Atomizers in a Combustor," Mechanical Engineer's Thesis, Massachusetts Institute of Technology, Cambridge, Massachusetts, 1978.
97. Wear, J.D. and Jones, R.E., "Comparison of Combustion Characteristics of ASTM A-1, Propane, and Natural-Gas Fuels in an Annular Turbojet Combustor," NASA Technical Note TN D-7135, January 1973.
98. Karpov, V.P. and Sokolik, A.S., "Ignition Limits in Turbulent Gas Mixtures," Proceedings of the Academy of Sciences of the USSR (Doklady Akademii (Nauk SSSR), Physical Chemistry Section, Volumes 139-141, 1961, pp. 866-869, Translated from Doklady Akademii Nauk SSSR, Volume 141, No. 2, November 1961, pp. 393-396.

1. Report No. NASA CR-3216		2. Government Accession No.		3. Recipient's Catalog No.	
4. Title and Subtitle <b>PREMIXING QUALITY AND FLAME STABILITY: A THEORETICAL AND EXPERIMENTAL STUDY</b>				5. Report Date December 1979	
				6. Performing Organization Code	
7. Author(s) Krishnan Radhakrishnan, John B. Heywood, and Rodney J. Tabaczynski				8. Performing Organization Report No. None	
				10. Work Unit No.	
9. Performing Organization Name and Address Massachusetts Institute of Technology Cambridge, Massachusetts 02139				11. Contract or Grant No. NGR 22-009-378	
				13. Type of Report and Period Covered Contractor Report	
				14. Sponsoring Agency Code	
12. Sponsoring Agency Name and Address National Aeronautics and Space Administration Washington, D. C. 20546					
15. Supplementary Notes Final report. Project Manager, Edward J. Mularz, U.S. Army R & T Laboratories (AVRADCOM), Propulsion Laboratory, Lewis Research Center, Cleveland, Ohio 44135. This report is based on a thesis submitted by the first author in partial fulfillment of the requirements for the degree Doctor of Philosophy to Massachusetts Institute of Technology in November 1978.					
16. Abstract Models for predicting flame ignition and blowout in a combustor primary zone are presented. A correlation for the blowoff velocity of premixed turbulent flames is developed using the basic quantities of turbulent flow, and the laminar flame speed. The correlation for blowoff velocity shows the correct trends for variations in equivalence ratio, flameholder characteristic size, free stream temperature and pressure, and turbulent Reynolds number. A statistical model employing a Monte Carlo calculation procedure to follow a chemical reaction through the course of a mixing process is developed to account for nonuniformities in a combustor primary zone. An overall kinetic rate equation is used to describe the fuel oxidation process. The model is used to predict the lean ignition and blow-out limits of premixed turbulent flames; the effects of mixture nonuniformity on the lean ignition limit are explored using an assumed distribution of fuel-air ratios. The model predictions of the flammability limits show the correct trends for variations in mixture temperature, pressure and velocity. With increased mixture nonuniformity, the model predicts a substantial reduction in the lean ignition limit. The trends in the model predictions are verified by experimental work on an atmospheric pressure constant cross-sectional area tubular combustor. Data on the effects of variations in inlet temperature, reference velocity and mixture uniformity on the lean ignition and blowout limits of gaseous propane-air flames are presented. The experimental work demonstrates that nonuniformities significantly reduce the lean ignition and blowout limits; however, nonuniformities substantially increase the emission levels of nitrogen oxides for lean mixtures.					
17. Key Words (Suggested by Author(s)) Flame stabilization; Premixed flames; Fuel-air nonuniformities; Blowoff velocity correlation; Modeling flame ignition and blowout; Prevaporizing, premixing combustors			18. Distribution Statement Unclassified - unlimited STAR Category 07		
19. Security Classif. (of this report) Unclassified		20. Security Classif. (of this page) Unclassified		21. No. of Pages 63	22. Price* A04